Charles University

Faculty of Science

Study programme: Medicinal Chemistry

Adam Cihlář

Synthesis of Chiral Sulfoxides and Their Applications

Syntéza chirálních sulfoxidů a jejich aplikace

Bachelor thesis

Supervisor: doc. RNDr. Jiří Míšek, Ph.D.

Prague, 2025

Prohlášení:

Prohlašuji, že jsem závěrečnou práci zpracoval samostatně a že jsem uvedl všechny použité informační zdroje a literaturu. Tato práce ani její podstatná část nebyla předložena k získání jiného nebo stejného akademického titulu.

V Praze, *09. 11. 2024*

Adam Cihlář

Acknowledgment

I wish to express my sincere gratitude to my supervisor, doc. RNDr. Jiří Míšek, Ph.D., for his invaluable guidance, insightful feedback, and for fostering my interest in the field both within and beyond the scope of this thesis. I am also appreciative of the entire team at Laboratory 007 for maintaining a collegial and light-hearted working environment. I am indebted to Mgr. Vladimír Nosek, Ph.D., for his expert advice on laboratory procedures, and to Pipatpon Raksapon, M.Sc., for his mentorship and open-minded approach. My thanks further extend to Mgr. Michal Urban, Ph.D., for performing the IR spectral measurements, and to RNDr. Martin Štícha, Ph.D., for conducting certain HRMS analyses. I also acknowledge the contributions of Ondřej Škrna and Martin Nováček in optimizing the geometry of target substrates for molecular docking as well as Lucie Němcová for providing valuable feedback in terms of stylistic and linguistic aspects of the thesis. Lastly, I am profoundly grateful to my family and friends for their unwavering support and encouragement, day and night.

Abstrakt

Chirální sulfoxidy nejsou pouze účinnými léčivy, ale také široce používanými ligandy a katalyzátory v asymetrické syntéze. Prvním cílem této práce byla syntéza chirálních sulfoxidů za účelem prozkoumání substrátové tolerance enzymu methionin sulfoxid reduktázy A (MsrA). Byla připravena řada chirálních sulfoxidů a identifikovány limitace týkající se různých variant MsrA. Druhým cílem této diplomové práce byla asymetrická syntéza benzoxazol chloromethyl sulfoxidu, který může sloužit jako univerzální chirální synthon pro přípravu chirálních sloučenin síry. Byl úspěšně syntetizován chirální ligand pro Mn(II)-katalyzovanou oxidaci a otestován v reakci s prochirálním sulfidem.

Klíčová slova: *Methionin sulfoxid reduktáza (MsrA), kinetická rezoluce, racemické sulfoxidy, asymetrická oxidace*

Abstract

Chiral sulfoxides are not only effective pharmaceuticals but also widely used ligands and catalysts in asymmetric synthesis. The first aim of this work was to synthesize a series of chiral sulfoxides to investigate the substrate scope of the enzyme methionine sulfoxide reductase A (MsrA). A range of chiral sulfoxides was prepared, and the limitations in the reactivity of various MsrA variants were identified. The second objective of this thesis was the asymmetric synthesis of benzoxazole chloromethyl sulfoxide, which can serve as a versatile chiral synthon for the preparation of chiral sulfur compounds. A chiral ligand for Mn(II)-catalyzed oxidation was successfully synthesized and tested in a reaction with a prochiral sulfide.

Key words: *Methionine sulfoxide reductase (MsrA), kinetic resolution, racemic sulfoxides, asymmetric oxidation*

Table of Content

1 State-of-the-art 8

1.1 Principal organic sulfoxides 8

1.2 MsrA 16

2 Principal aims of the thesis 22

3 Results and discussion 23

3.1 Synthesis of racemic sulfoxides with various substituents 23

3.2 Kinetic resolution of sulfoxides 26

3.3 Development of a novel general method for asymmetric synthesis of sulfoxides 29

4 Experimental section 34

4.1 General procedure 34

4.2 Synthesis of p-tolyl sulfoxides 35

4.3 General procedure for kinetic resolution of sulfoxides with MsrA 40

4.4 Asymmetric oxidation of benzoxazole-containing sulfoxides 41

5 Conclusion 46

6 Use of Artificial Intelligence 47

7 Literature 48

Used Abbreviations

Ac – acetyl

AUC – area under curve

BINOL – binaphthol

Boc – tert-butyloxycarbonyl

Cys, C – cysteine

COVID-19 – Coronavirus disease 2019

DABSO – 1,4-diazabicyclo[2.2.2]octane bis(sulfur dioxide)

DCE – dichloroethane

DET – diethyl tartrate

DmsABC – dimethyl sulfoxide reductase

DMSO – dimethyl sulfoxide

DTNB – 5,5′-dithiobis-(2-nitrobenzoic acid)

DTT – dithiothreitol

EDC – 1-ethyl-3-(3-dimethylaminopropyl)carbodiimide

ee – enantiomeric excess

Et – ethyl

EtOH – ethanol

FDA – Food and Drug Administration

Fp – hexafluoro-2-propanol

frMsr – free methionine-sulfoxide-reductase

GERD – gastroesophageal reflux disease

Glu, E – glutamic acid (glutamate)

GSH – glutathione

h – hour(s)

HIV – human immunodeficiency virus

HPLC – high performance liquid chromatography

HOBt – hydroxybenzotriazole

HRMS – ligh-resolution mass spectrometry

IBX – 2-iodoxybenzoic acid

IC50 – half maximal inhibitory concentration

iPr – isopropyl

IR – infrared spectroscopy

LRMS – low-resolution mass spectroscopy

Me – methyl

min – minute(s)

MsrA – methionine-sulfoxide-reductase A

MsrB – methionine-sulfoxide-reductase B

mCPBA – meta-chloroperbenzoic acid

NADPH – nicotinamide adenine dinucleotide phosphate

NaH – sodium hydride

NMR – nuclear magnetic resonance

NSAID – non-steroidal anti-inflammatory drug

Ph – phenyl

PCR – polymerase chain reaction

PMSO – protein-bound methionine sulfoxide

PPI – proton pump inhibitor

R – rest of molecule

(R-) – rectus

ROS – reactive oxygen species

(S-) – sinister

SAM – S-adenosylmethionine

TBAF – tetrabutylammonium fluoride

TBHP – tert-butylhydroperoxide

tBu – tertbutyl

TCEP – tris(2-carboxyethyl)phosphine

TEAB – tetraethylammonium bromide

TEMPO – (2,2,6,6-tetramethypiperidine-1-oxyl

TES – triethylsilyl

Tf – trifluoromethanesulfonyl

TFA – trifluoroacetic acid

THF – tetrahydrofuran

TIPS – triisopropylsilyl

TLC – thin layer chromatography

TMS – trimethylsilyl

TRIS – tris(hydroxymethyl)aminomethane

Trp, W – tryptophane

Tyr, Y – tyrosine

TsO – p-toluensulfonyl

UV/Vis – ultraviolet-visible spectroscopy

WT – wild-type

1 State-of-the-art

1.1 Principal organic sulfoxides

Sulfoxides, alternatively sulfoxides, are organic compounds containing a sulfinyl functional group SO attached to two adjacent carbons. Together with sulfides, sulfones and corresponding sulfenic, sulfinic and sulfonic acids they form a diverse chapter in organic chemistry (Figure 1).

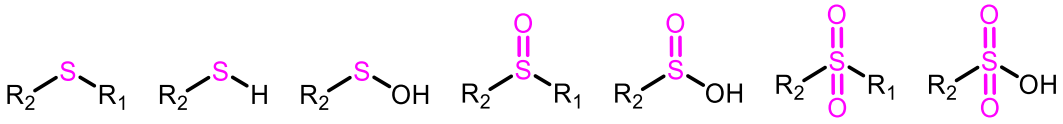

Figure 1: Important sulfur-containing functional groups, from left to right: sulfide, thiol, sulfenic acid, sulfoxide, sulfinic acid, sulfone, sulfonic acid.

Sulfoxide group bears certain resemblance to the carbonyl one, with C-O and S-O bonds being of similar distances.[1,2] Tetrahedral geometry of the sulfinyl group has led to debate about the electronic nature of the S=O bond, commonly explained by the interaction between oxygen's 2p orbital (donating) and sulfur's 3d orbital (accepting) in a d – p_π bonding.[3] Consequently, it has been proven that the S=O bond is only partially double in order. Sulfoxides also exhibit considerable polar behaviour, being more polar than sulfides or sulfones. This fact, together with the specific bond properties, has led to sulfoxide moiety being represented through ionic resonance structures (though covalent structures can also be found). Provided both side chains are unsymmetrical, a chirality centre is present on the central sulfur atom, with an inversion barrier of 35 – 43 kcal/mol and racemization temperatures well above 200 °C for aromatic compounds.[4,5] This makes optically active sulfoxides abundant not only in synthetic chemistry but also in live organisms.

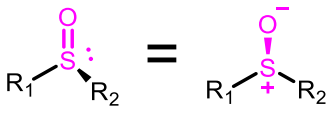

Figure 2: Different representations of chirality in the sulfoxide group.

While smaller molecules such as dimethyl sulfoxide find their steady use as solvents in organic chemistry or biochemistry, sulfoxide motives are most notably found in biologically active

compounds and intermediates in organic synthesis, where their value as useful synthons is crucial.

1.1.1 Biologically active sulfoxides

Numerous pharmaceuticals having a sulfoxide moiety exist, ranging from proton pump inhibitors to anti-inflammatory medication. Quite interestingly, despite being the most primitive sulfoxide, DMSO finds large use in medicine despite its reputation as a common solvent in organic chemistry and cell biology. While FDA approval has been granted solely for the treatment of interstitial cystitis, DMSO is present in numerous transdermally applied pharmaceuticals, increasing their bioavailability.[6] It has also been widely used in alternative medicine. While toxicity of DMSO is considered low, new research has suggested cytotoxic effect, with considerable disruption in cellular processes.[7,8] Another sulfoxide with a diphenyl and amidic groups, modafinil, is used as a treatment for narcolepsy and other sleep disorders (Figure 3). Recently, it has been subject to extensive study due to its low abuse potential and immunomodulatory effects.[9] It has also been used as a nootropic. Sulindac (**1**), belonging to group of NSAIDs, is centred around its indene motif (with the name being derived from **sul**finyl, **ind**ene and **ac**etic acid). Despite being on the market for more than 50 years, little further research has been done on improving its capabilities. Recently, new variants of the drug were synthesized and exhibited increased anti-inflammatory activity, though their analgesic properties remained the same.[6] Further research on these compounds has revealed that optically active variants present better pharmacokinetic properties coupled with fewer side effects.[10] R-modafinil (Armodafinil, **2**) demonstrated better bioavailability, with higher c_{max} and AUC values than its racemic analogue.[11]

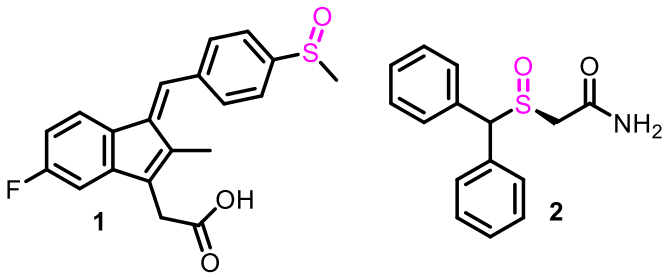

Figure 3: Sulindac (**1**) as a racemic mixture and armodafinil (**2**).

Intensive inquiry into the properties of optically active sulfoxides has led to the development and discovery of a plethora of compounds. Chemokine receptor inhibitor Cenicriviroc (**3**), an

experimental anti-HIV drug, has also been tested as an anti-inflammatory agent against COVID-19.[6] YM-38336 (**4**, a spiro-substituted piperidine) proved to be a selective neurokinin receptor antagonist, with its optically active variant (*R-, R-*) demonstrating better selectivity and lower IC_{50}.[12–14] Numerous optically active compound bearing a sulfoxide moiety also exist in nature. Cyclic fungal tetrapeptides ustiloxins (**5**), produced by fungus *U. virens*, serve as cytostatic agents, with potential use being investigated in cancer treatment. Antibiotic sparsomycine (**6**) functions as a protein synthesis inhibitor, much in the same way as Chloramphenicol. (*R)*-Sulforaphane (**7**), found in cruciferous vegetables such as cabbage, positively modulates phase II metabolization enzymes.[15] Lastly, present in *Amanita* species, cyclic peptides amatoxins constitute one of the most potent toxins in the animal kingdom, with α-amanitin (**8**), isolated from *Amanita phalloides*, having a lethal dose of 100 µg/kg.[16]

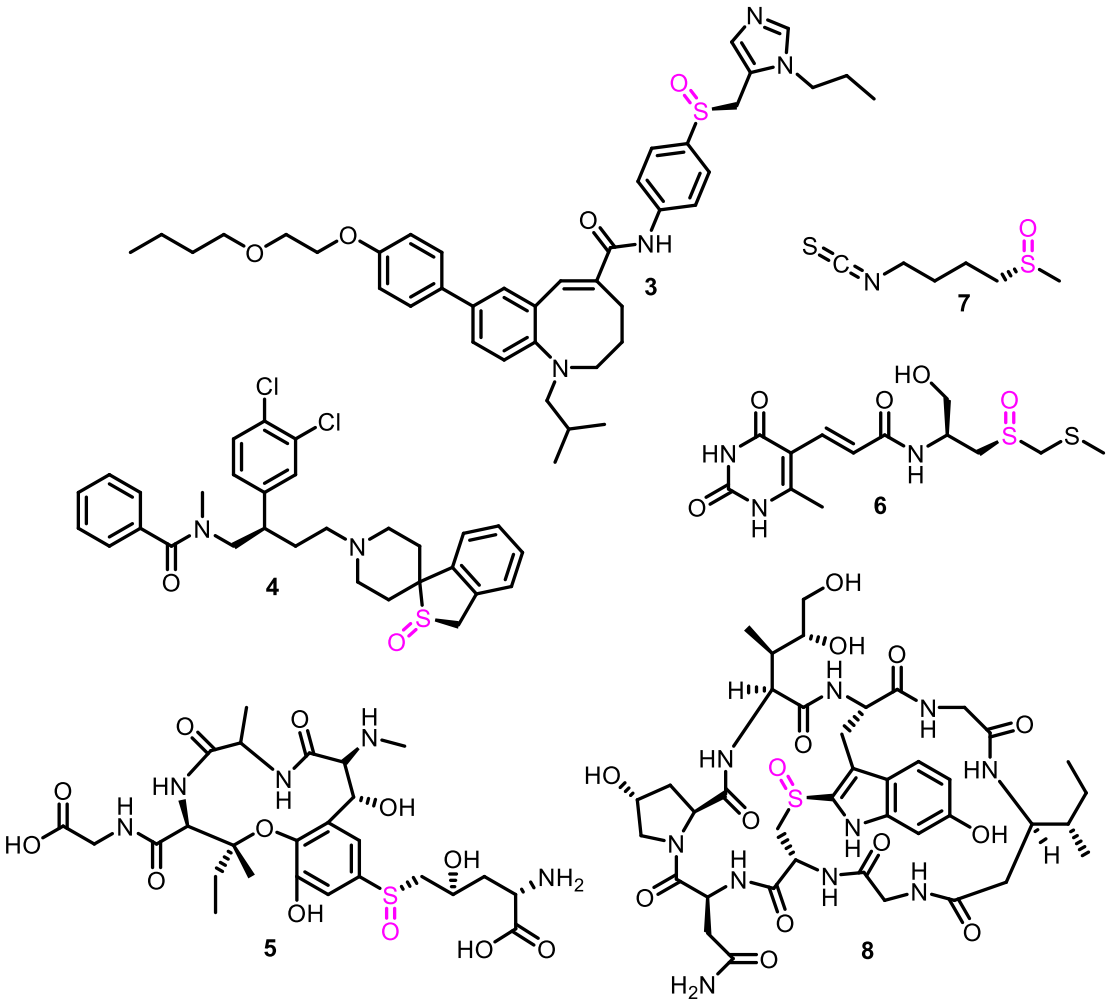

Figure 4: Optically active sulfoxides. **3**: Cenicriviroc. **4**: YM-38336. **5**: ustiloxin A. **6**: sparsomycine. **7**: *(R)*-sulforaphane. **8**: α-amanitine.

1.1.1.1 Proton pump inhibitors (PPIs)

PPIs are a class of drugs that serve to relieve peptic ulcers and gastroesophageal reflux disease (GERD). They are based on the common framework of prazole – a sulfoxide with benzimidazole and pyridine fragments (Figure 5).

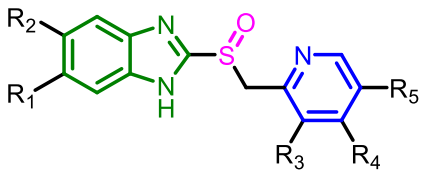

Figure 5: Prazole with its benzimidazole moiety (green) and pyridine moiety (blue).

Four most famous representatives of PPIs are omeprazole **12**, rabeprazole **10**, lansoprazole **9** and pantoprazole **11**. They are also available as optically pure variants (esomeprazole **12** or dexlansoprazole **9**). Though both racemic and optically pure mixtures have same efficiency (active metabolite is achiral), optically pure ones demonstrated better pharmacokinetic parameters (AUC of esomeprazole was up to 7 times higher than that of omeprazole).[17] In recent days, this fact has been called into question, though there is no scientific consensus on the issue.[6] There have also been studies that suggested possible negative side effects associated with chronic use – though studies that have reached a contrary result exist as well. Figure 6 shows the most notable proton pump inhibitors.

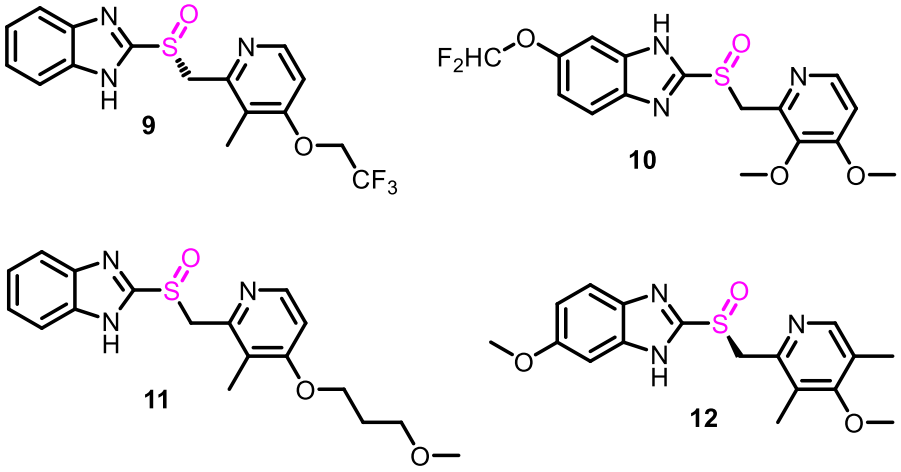

Figure 6: **9**: Dexlansoprazole; **10**: Rabeprazole; **11**: Pantoprazole; **12**: Esomeprazole.

1.1.2 Synthesis of sulfoxides

Multiple ways of sulfoxide synthesis exist. Experiments utilizing thionyl chloride and acylchlorides were among the first reported procedures for synthesis of both symmetrical and unsymmetrical sulfoxides.[18] Additionally, reaction of sulfinates and carbonyls containing an α-acidic hydrogen can also be used. Sulfinamides have been shown to be suitable substrates for asymmetrical synthesis of sulfoxides, as demonstrated by Wudl.[19]

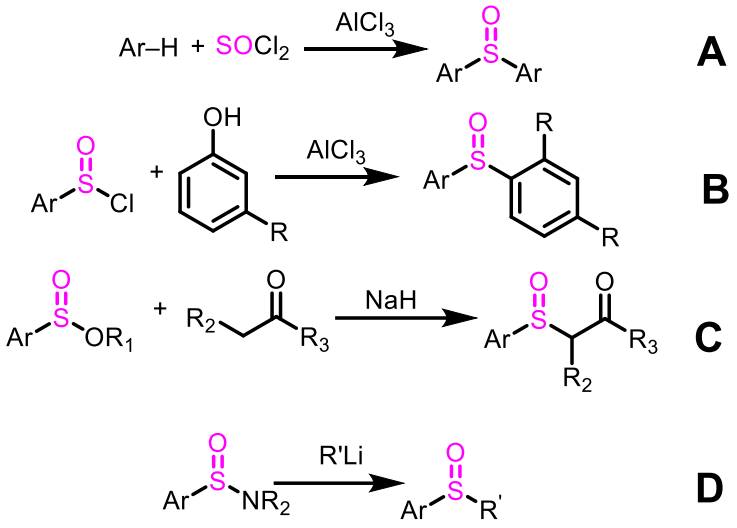

Figure 7: (**A**): Synthesis of diaryl sulfoxides using thionyl chloride. (**B**): Synthesis of unsymmetrical sulfoxides using Chasar's and Pratt's technique. (**C**): Synthesis of modified sulfoxides by reacting substituted sulfinates with alfa-carbonyl compounds. (**D**): Synthesis of sulfoxides by implementing organolithium compounds and sulfinamides.

Grignard reagents also play a crucial role in synthesis of sulfoxides.[20] While initially having been used in reaction with acyl chlorides (Fig. 8,**C**), subsequent experiments have investigated different mechanisms (Fig. 8, **A**,**B**) for enhanced regio- and stereoselectivity.[21–23] As a result, newly developed one-pot syntheses have created effective reagents, which allow for milder conditions and improved reaction time, such as DABSO (**13**) or sulfoxide **14**.

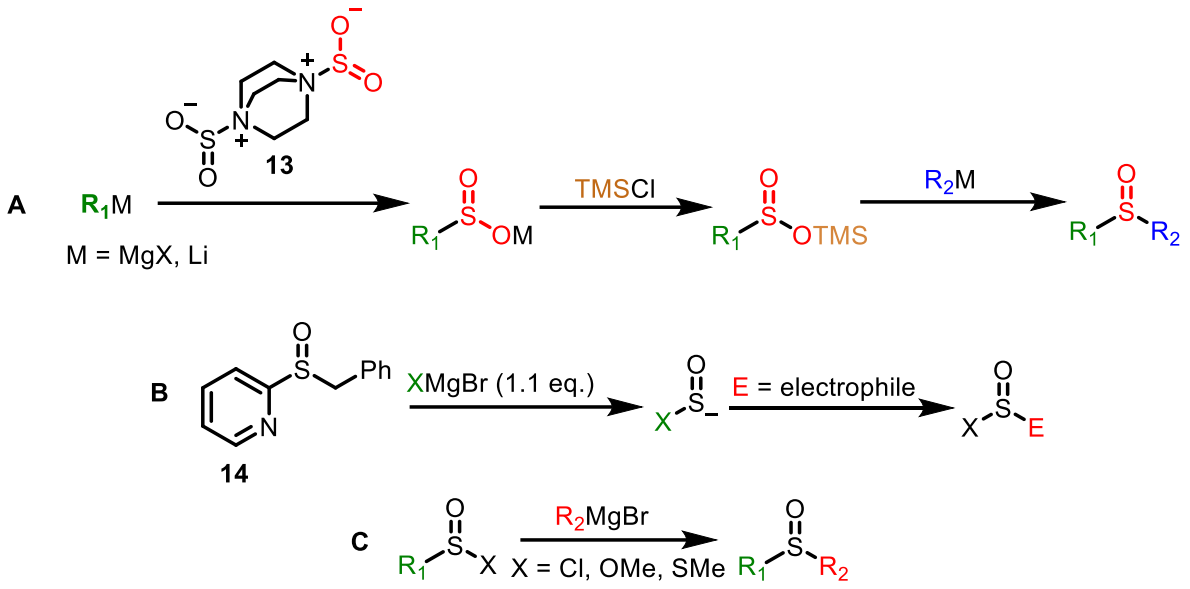

Figure 8: Synthesis of unsymmetrical sulfoxides utilizing organometal reagents.

Interestingly, Grignard reagents have also been used in reaction with chloromethyl sulfoxides, generating aryl an alkyl products in high yields and selectivity.[24] Contrary to first belief, chloromethyl group has proven to be a viable leaving group, with *p*Ka between ranges of 25-30. Grignard reaction provokes pyramidal inversion at the chirality centre leading to the retention of enantiomeric purity.[25]

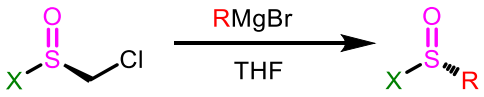

Figure 9: Synthesis of sulfoxides by means of reacting chloromethyl sulfoxides with Grignard reagents.

Another route for effective sulfoxide synthesis resides in oxidation of sulfides to corresponding sulfoxides.[20] Compounds such as hydrogen peroxide, *m*-chloroperbenzoic acid (mCPBA) or tert-butyl hydroperoxide (TBHP) have become standard choice for oxidative synthesis of sulfoxides (Fig. 10, **A**,**D**) from sulfides due to their modest cost and optimal oxidation potential. However, peroxo- compounds tend to suffer with poor chemoselectivity, often yielding a mixture of products. As such, effort has been made to develop chemoselective oxidation methods. Hydrogen peroxide coupled with hexafluoro-2-propanol ("fluorous phase") has shown considerably high yields, the same can be said for $TiCl_3$.[26] Halogen-based oxidants such as combination of TEMPO/NaOCl (Fig. 10, **B**, 2,2,6,6-tetramethypiperidine-1-oxyl) or IBX (Fig. 10, **C**) have demonstrated chemoselective oxidation even in sensitive compounds.[20]

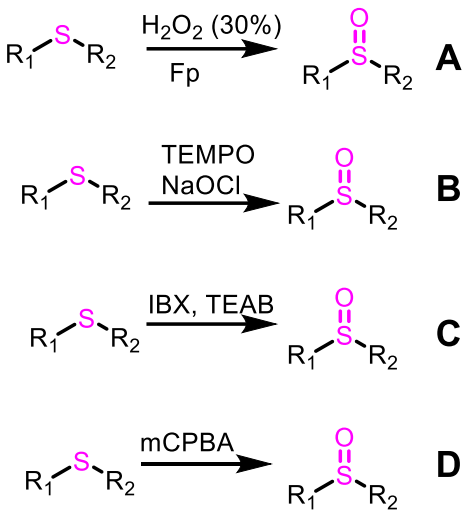

Figure 10: Oxidative syntheses of sulfoxides. (**A**): Oxidation with hydrogen peroxide in fluorous phase (Fp). (**B**): conversion via use of sodium hypochlorite and TEMPO with high chemoselectivity. (**C**): Catalysis using o-iodoxybenzoic acid (IBX) with tetraethylammonium bromide (TEAB). (**D**) Oxidation using mCPBA as a common procedure.

Several asymmetrical procedures have been devised over the years, mainly to pursue growing demand for enantiopure pharmaceuticals and intermediates in organic synthesis. In the 1980s, Kagan and Modena independently developed asymmetrical oxidation methods by using Ti(Oi-Pr)$_4$ as a catalyst and diethyl tartrate as a chiral ligand (Figure 11).[27,28] Further methods have been consequently developed, using different catalysts in tandem with Ti(Oi-Pr)$_4$ such as binaphtol (BINOL) in Uemura oxidation or modified tartrate ligands as in Gao oxidation.[29,30] To this day, major pharmaceuticals such as esomeprazole are synthesized using modified variants of Kagan procedure.[31]

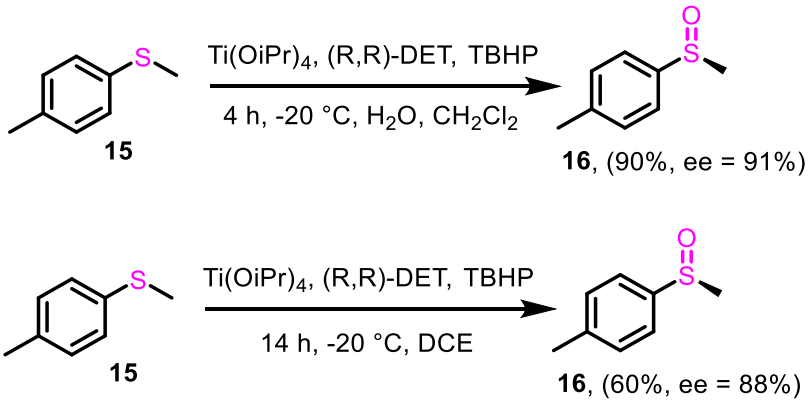

Figure 11: Kagan (top) and Modena (bottom) procedures as a means of chiral sulfoxide synthesis.

Besides titanium, catalysts utilizing other metals such as manganese and vanadium exist (Figure 12). The former is stabilized by ligands belonging to the class of Salen/Salan system, as demonstrated by the Katsuki oxidation (**22**).[32,33] Recently, Salen/Salan-inspired manganese catalysts, utilizing hydrogen peroxide, have been developed by Dai et al., with great success for a wide range of sulfides.[34]

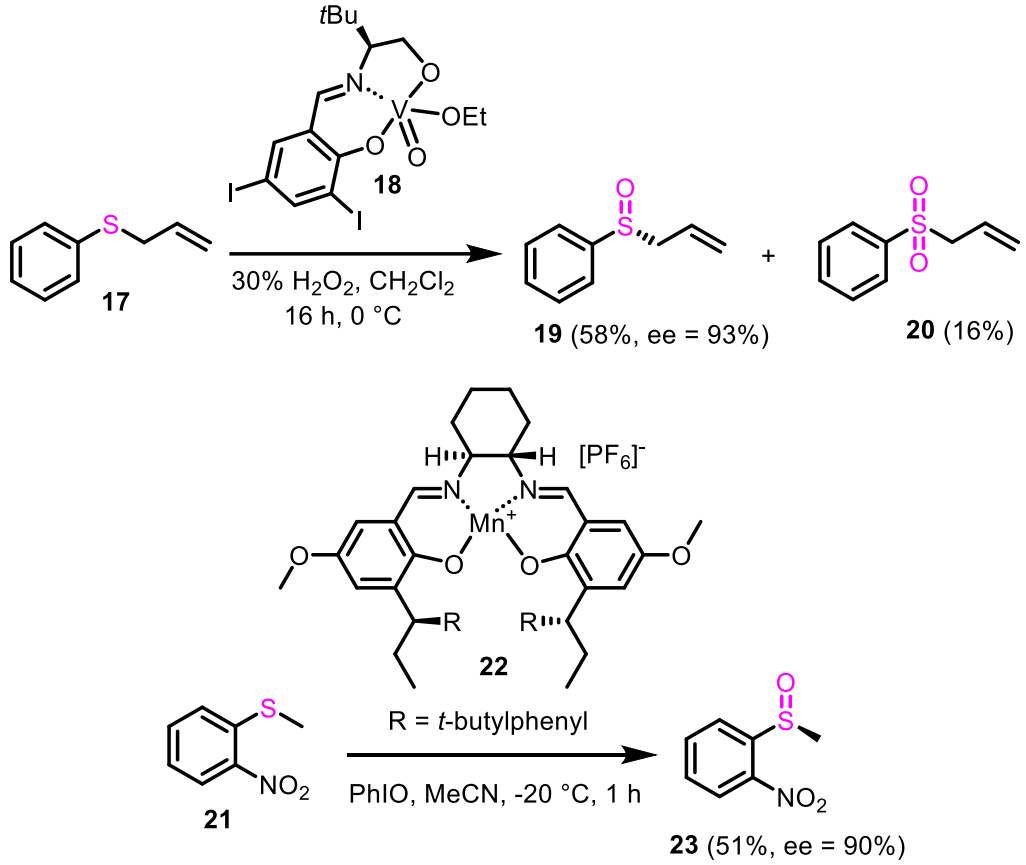

Figure 12: Vanadium catalysts (**18**) and manganese catalysts (**22**) demonstrate enantioselective and chemoselective properties when oxidating arylsulfides.

Interestingly, with scientific breakthroughs having been achieved in the field of biocatalysis, an alternative to often expensive and environmentally unfriendly metal-catalyst-utilizing reactions in the form of enzymatic preparation of chiral sulfoxides has been investigated in recent years.[35] Most notably, means of directed evolution, utilizing techniques such as error-prone PCR, have yielded enzymes with enhanced biocatalytic properties.[36–38] This can be demonstrated on a mutant variant of bacterial lipase from *Pseudomonas aeruginosa*, with the mutant variant demonstrating an increased selectivity for natural substrates (Figure 13).[39]

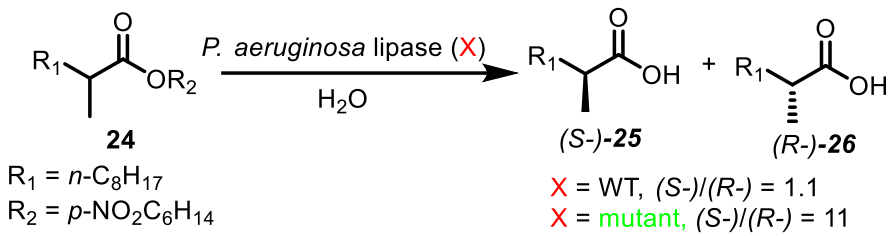

Figure 13: Directed evolution of bacterial lipase as a means of enantioselectivity increase.

One particular group, sulfoxide reductases, has been shown to reduce not only biological, but synthetic substrates, with considerable reactivity.[40] Further studies have expanded on this fact, widening the scope of susceptible compounds and developing new ways for improved conversion.[41,42] Though this field provides an alternative to conventional asymmetrical methods, it has yet to resolve major drawbacks for industrial application. Deracemization techniques have so far rarely provided yields above 50 % and it has been found that higher substrate concentrations detrimentally impact the enzyme's activity.[42]

1.2 MsrA

Methionine sulfoxide reductase A is a naturally occurring mitochondrial enzyme that catalyses the conversion of S-methionine sulfoxide into S-methionine. Furthermore, it is selective only to the (*S*)-sulfoxide stereoisomer. Different isoforms of the enzymes, called MsrB and frMsr, exhibit different behaviour, with MsrB reducing only the (*R*)-sulfoxide stereoisomer of the methionine sulfoxide and frMsr being present in unicellular organisms.[43] Furthermore, two variants of human MsrA exist: a long variant, which has an extra N-terminal mitochondrial targeting sequence, an a short variant, which lacks such chain.[44]

The structure of MsrA is largely similar among species, with variants retaining their catalytic site and core features, and differing in molecular weight (while the human variant has a molecular weight of 26 kDa, the *E. coli* variant has only 23 kDa).[45] The globular tertiary structure, formed largely by alfa-helix and beta-sheet motives, contains a substrate-binding pocket utilizing amino acids glutamate (Glu, E), cysteine (Cys, C), tyrosine (Tyr, Y), phenylalanine (Phe, F) and tryptophan (Trp, W). The cysteine in the sequence is part of a cysteine triarchy required for catalytic function, consisting of C51, C198 and C206 (Figure 14).[46]

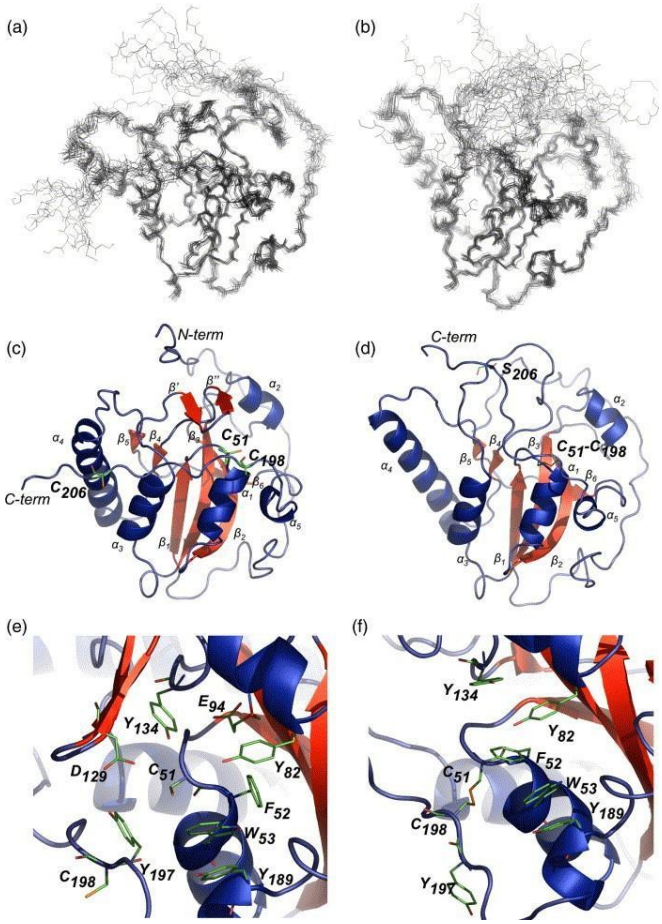

Figure 14: Structure of reduced and oxidized MsrA. (a) and (b) show backbone structure, (c) and (d) show secondary structure with marked cysteine triarchy, (e) and (f) show the active site.[46]

The catalytic mechanism of MsrA could be first described by stabilization of the substrate in the enzymatic cavity (**I**) via Y82, E94 and also Y134, followed by nucleophilic attack of C51 (**II**) to form an intermediate (**IV**) (Figure 15). Subsequently, catalytic cysteine residue is attacked with water, releasing the sulfide molecule (**V**) and forming a corresponding disulfide with C198 (**VI**). The enzyme is regenerated with a thioredoxin/NADPH system in cellular environment or by common reducing agents such as DTT or TCEP in vitro (**VII**). It should also be noted that other amino acids present in the active site (F52, W53 and others shown in Figure 14) also facilitate the catalytic process, stabilizing the substrate.[47]

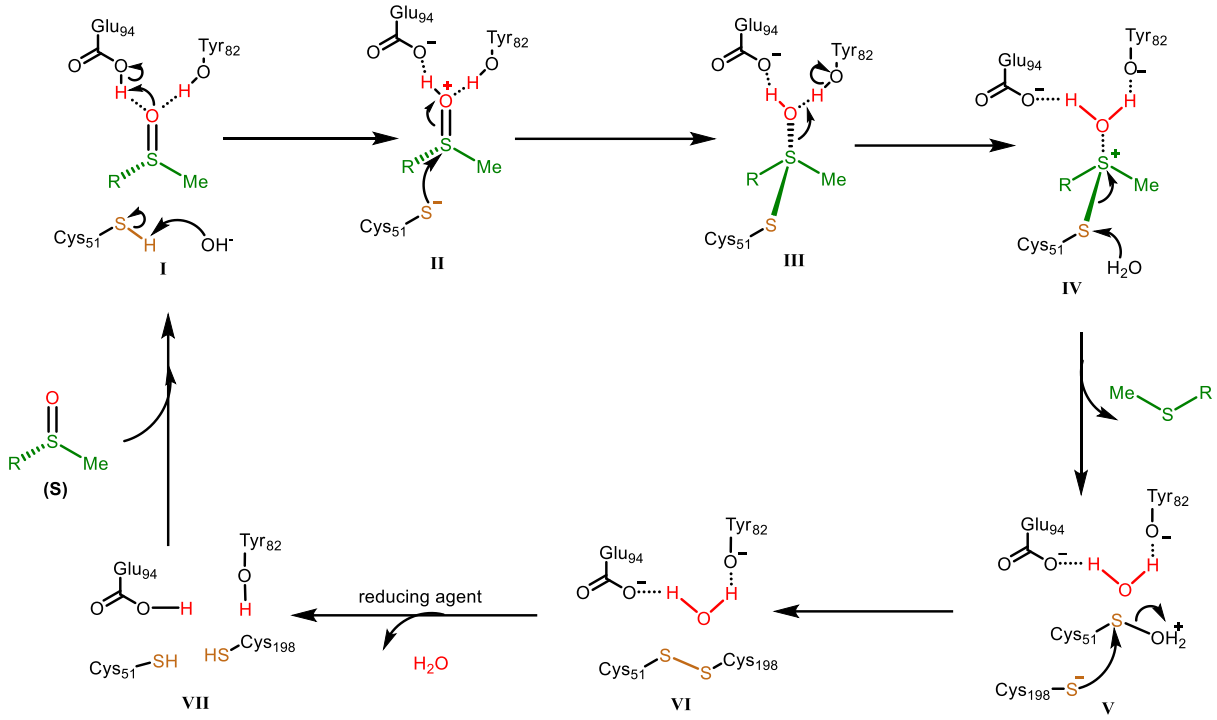

Figure 15: Proposed mechanism of action of reducing capabilities of MsrA.

1.2.1 Function of MsrA

The main consequence of MsrA function as a methionine-sulfoxide reducer is its indirect protection against reactive oxygen species (ROS) such as peroxide, superoxide and hydroxyl radicals. Methionine is easily sensitive to oxidation and studies have shown that both outside and inside sources of ROS directly influence methionine oxidation.[48] Furthermore, absence of the enzyme increased susceptibility to oxidative stress in both primitive and complex organisms.[49] These findings go hand in hand with the fact the MsrA is found in the inner mitochondrial membrane, taking part in the respiratory complex. Increased oxidative stress oxidizes cysteine in cytochrome c and impacts the cascade.[50] Though the exact role of MsrA in mitochondrial regulation is not understood, current information points out to its considerable importance.

Reduction of methionine-sulfoxide by MsrA is not unique to free methionine – MsrA works on protein-bound methionine-sulfoxide (PMSO) as well. An example of this function can be demonstrated on substrate alfa-crystallin, a lens-bound protein which serves as a heat shock protein. Studies have shown that oxidized methionine in alfa-crystalline greatly decreases functional capability of the protein.[51] Protective properties of MsrA can be demonstrated on a

wide array of other substrates, including calmodulin, HIV-2 protease and shaker potassium channel.[50] Figure 16 is a schematic representation of MsrA protective capabilities.

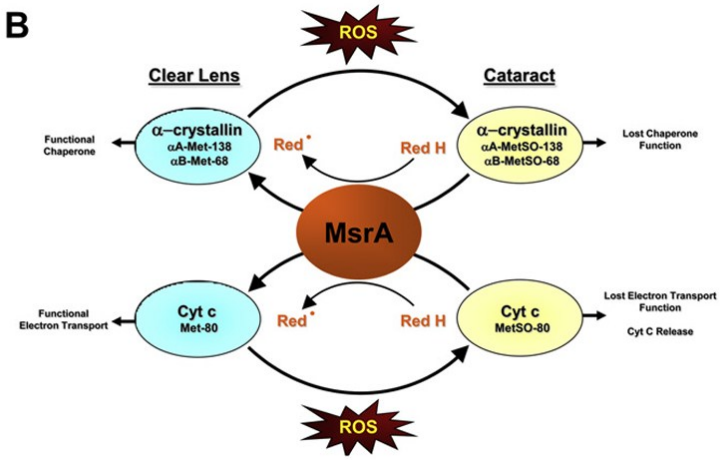

Figure 16: Sulfur-containing proteins cytochrome c and alfa-crystalline are oxidized to corresponding sulfoxides with ROS. Catalytic properties of MsrA regenerate the active forms of these proteins.[50]

It should also be noted that methionine-sulfoxide (both free and protein-bound) can undergo further oxidation to a corresponding sulfone. All variants of Msr are unreactive with this substrate, rendering the oxidation virtually irreversible in biological systems.

1.2.2 MsrA Applications

Studies have shown that levels of MsrA, together with MsrB, decrease with age.[52] Additionally, there was evidence to suggest that MsrA plays a role in certain diseases such as Alzheimer's. Even though understanding of MsrA role in aging and degenerative disease is low, there is evidence to suggest that further research will bring productive results. Previous methods relied on developing an antibody-detecting system for methionine-sulfoxide (a sign of increased oxidative stress), though with little success. Additionally, modulation of MsrA and MsrB activity could influence sulfur metabolism. While methionine is an essential amino acid, cysteine is not and can be synthesized from the former. Through a complex regulation cycle involving substances such as S-adenosyl-methionine (SAM), common disease marker homocysteine and glutathione (GSH), MsrA regulates not only the formation of other sulfur-containing compounds, but also other important antioxidants (namely GSH). It is also further evidence to support the link between aging and MsrA activity (increased age correlates with higher levels of homocysteine).[52]

MsrA activity has also been reported in metabolism of drugs containing different sulfoxide motives. Methyl-sulfinyl drugs such as sulindac (**27**, NSAID), mesoridazine (**28**, treatment of schizophrenia) or triclabendazole (**29**, common treatment for liver fluke) are directly metabolized by MsrA, with triclabendazole's efficiency being a direct result of MsrA activity.[52] Further drugs affected by MsrA also include uricosuric Sulfinpyrazone (Figure 17**).**

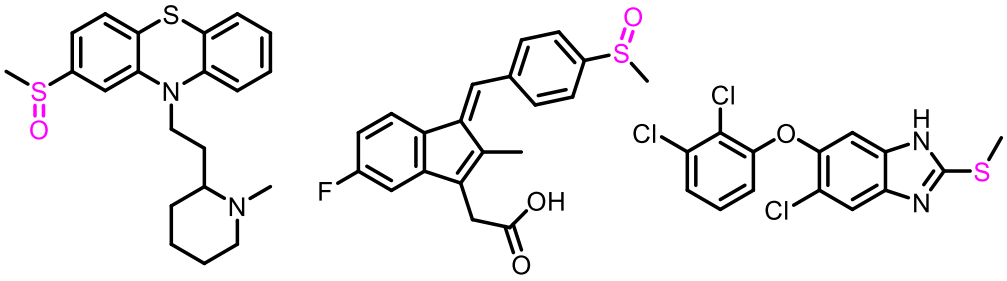

Figure 17: Methyl-sulfinyl drugs mesoridazine, sulindac and triclabendazole (shown in its sulfide form, though the oxidated version is biologically active).

Enantioselective reduction of pharmaceuticals has prompted researchers to utilize MsrA in other fields, particularly enantioselective synthesis and biocatalysis. Numerous studies by Míšek et al. investigated the substrate scope of several sulfur-based oxidoreductases. Substituted aromatic methylsulfoxides have been prone to MsrA activity with both considerable yields and enantiomeric excess (ee).[53,54] Having observed the substrate-scope of the enzyme, they have utilized directed evolution techniques to create a new enzyme variant of MsrA (F52L). Surprisingly, the mutant variant tolerated wider range of substrates, particularly substitution of the methyl group for larger alkyl chains (*Table 1*). This enabled for an efficient kinetic resolution of albendazole-sulfoxide (a metabolite of antiparasitic albendazole).[55]

Table 1: Investigation of sulfur oxidoreductases MsrA (with its wild-type variant Wt and developed mutant F52L) regarding their activity on different racemic sulfoxides. Reaction conditions were as follows: Wt, F52L: substrate (1 eq.) with DTT (4 eq.) and enzyme (0,5 mol%) in PBS buffer for 24 h at 25 °C; n.d. = not determined.

Entry	Substrate	Wt conversion; ee [%]	F52L conversion; ee [%]
1	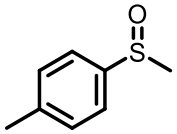	50; 99	50; 99
2	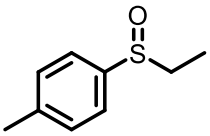	50; 99	50; 99
3	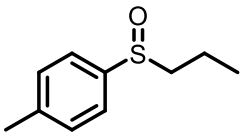	<3; n. d.	50; 99
4	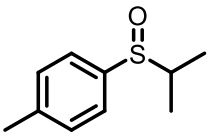	<3; n. d.	<3; n. d.
5	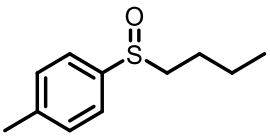	<3; n. d.	50; 99
6	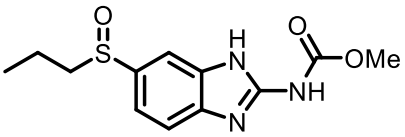	6; 6	49; 94

2 Principal aims of the thesis

The experimental part can be structured into the following categories:

1. Synthesis of a series of racemic sulfoxides and a subsequent enzymatic assay to investigate the substrate scope of the new MsrA variant F52L.
2. Development of an asymmetric synthesis of benzoxazole chloromethyl sulfoxide and subsequent application.

3 Results and discussion

3.1 Synthesis of racemic sulfoxides with various substituents

Our group has previously pioneered new experiments surrounding sulfoxide reductases.[53–55] Based on our findings, MsrA does prove to be a viable biocatalyst with both enantioselective and chemoselective properties. However, the substrate scope of wild-type enzyme remained relatively low, effectively being reduced to sulfoxides bearing methyl and ethyl moiety. This has led our laboratory to devise a new variant of the enzyme, F52L by means of directed evolution. The mutant variant (F52L) had demonstrated improved reactivity for bulkier aliphatic groups (such as propyl or butyl) on the side chain. However, the substrate scope of the new variant has not been thoroughly investigated. One of the aims of this thesis was to define limitations of the catalytic activity of the new F52L MsrA variant. Therefore, sulfoxides with longer aliphatic chains, different carbon hybridization and heteroatom substitutions were designed to probe the enzyme substrate specificity (Figure 18). To grasp the sterical limitations of the active site, sulfoxides **32** and **34** with pentyl and hexyl group respectively were chosen as the starting substrates and synthesized.

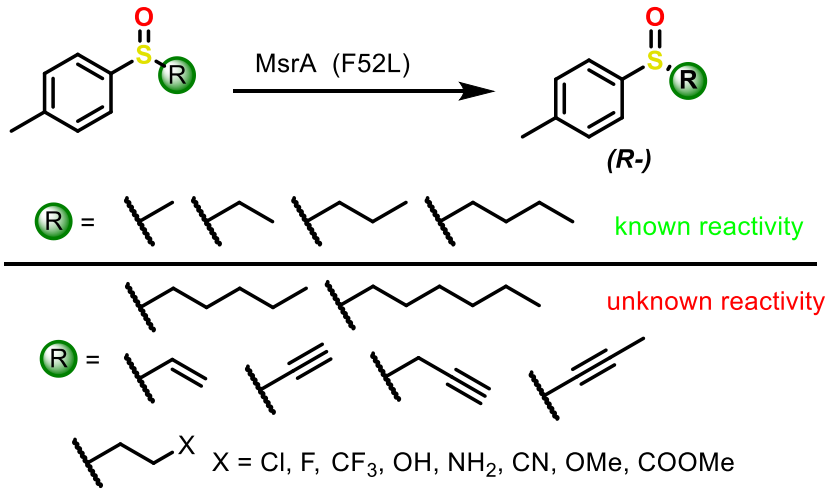

Figure 18: Schematic representation of investigated substrate scope of an MsrA variant F52L and planned experiments regarding its catalytic activity.

Synthesis of sulfoxide **32** started with thiol **30** which was alkylated with pentylbromide in the presence of NaOH, giving sulfide **31** (87%). It should be mentioned that during TLC analysis, intermediate **31** proved to have the same R_f as thiol **30**. Consequently, conversion of **30** had been monitored using Ellman's reagent. The intermediate **31** was then oxidized using hydrogen

peroxide in acidic conditions providing the target sulfoxide **32** in good yield (82%). This oxidation method provided minimal overoxidation of sulfoxide **32** to sulfone, which is a common side reaction with reagents like mCPBA. Hexyl sulfoxide **34** had been prepared using the similar procedure as **32**. Ellman's reagent had also been used for TLC visualization. Yields corresponded to those of **31** and **32** (Figure 19).

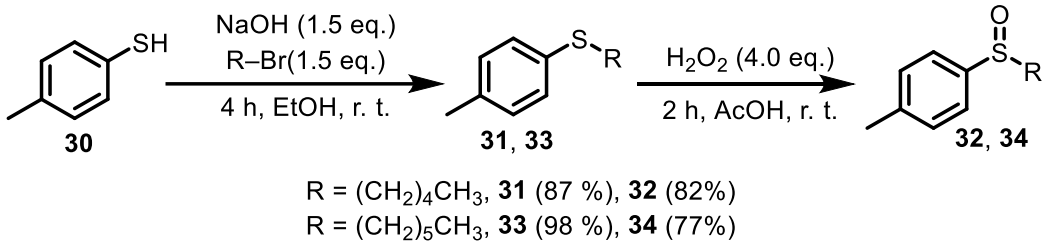

Figure 19: Synthesis of alkylarylsulfoxides **32** and **34**.

We and others have observed that ethyl and ethenyl sulfoxides are good substrates for wt MsrA. We wanted to assess if ethynyl substituent with different hybridization and rigidity would be also tolerated by the enzyme. Therefore, synthesis of ethynylsulfoxide **40** was devised (Figure 20). Sodium sulfinate **35** had been converted to the corresponding sulfinylchloride **36** using $SOCl_2$, followed by a reaction with lithium ethynyltriisopropylsilane. The resulting product **37a**, obtained in the modest yield of 21%, had been subjected to TBAF-mediated deprotection of the alkyne. However, this decisive step provided a complex mixture of products.

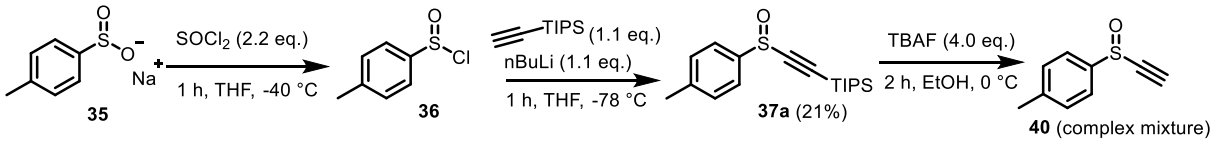

Figure 20: Attempted synthesis of ethynyl sulfoxide **40**.

Based on this information, a different approach had been suggested, first converting **35** into its methylester form **38** to ensure a stable starting compound. Different acetylidation techniques had been tried out to as it is exemplified in *Table 2*.

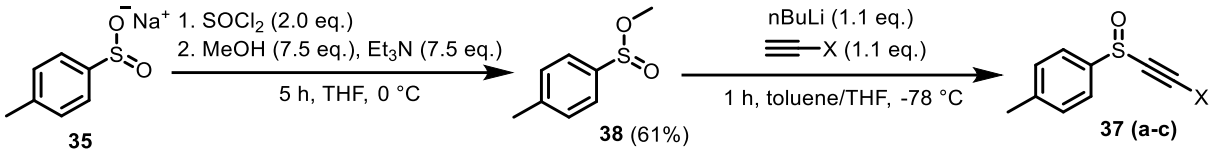

Table 2: Optimalization of synthesis of ethynyl sulfoxides **37** from sulfinate **35**.

Product	Conditions	Solvent	Yield [%]
37b	nBuLi (1.1 eq.) TES (1.1 eq.)	THF	<10
37c	nBuLi (1.1 eq.) TMS (1.1 eq.)	THF	<10 (complex mixture)
37c		Toluene	27
40	MgBr (1.1 eq.)	THF	<5 (complex mixture)
40		Toluene	<5 (complex mixture)

As *Table 2* demonstrates, the reaction of methylester of **38** with methynyltrimethylsilane in presence of nBuLi in dry toluene provides clear product **37c**, though in lower yields. Different approaches were also evaluated in deprotecting the silane group, with the best conditions being obtained by potassium fluoride (4 eq.) and a 5% mixture of water in ethanol at room temperature (Figure 21).

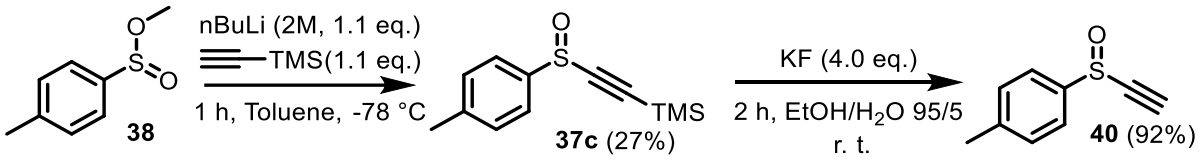

Figure 21: Synthesis of **37** as a result of reaction optimization.

Though Figure 21 showcases a viable synthesis path towards **40**, the yields of corresponding reactions could use further optimization. Reverse addition of reactants leading to compound **37c** had also been tried out, though with no effect. It has also been noted that **40** tended to decompose even when stored under inert atmosphere and low temperatures (4-6 ° C).

We wanted to investigate the effect of heteroatom substitution on the sulfoxide substituent to further analyse the enzyme's substrate scope. To this amount, aminosulfoxide **44** was prepared via reaction of **30** and tosylate **41**, followed by oxidation using hydrogen peroxide in acidic conditions and Boc deprotection using TFA (Figure 22). Sulfide **42** was obtained in a lower

yield than was expected (63%) which had probably been caused by losses following purification on silica. Sulfoxide **43** had also been obtained in similar yields (66%) with the substrate **42** having had lower reactivity than sulfides **31** and **33**. Reaction of sulfoxide **43** with TFA after 4 hours gave amine **44** with TLC showing total conversion. Silica column chromatography proved to be an unsuitable method for purification as it yielded a mixture of amine **40** and triethylamine/TFA salt (triethylamine had been part of the eluent mixture). HPLC yielded amine **40** as a TFA salt in 80 % yield.* The product also demonstrated remarkably high polarity, not dissolving in cyclohexane, dichloromethane or ethyl-acetate. Recrystallization could prove to be a viable alternative, though it had not been tested.

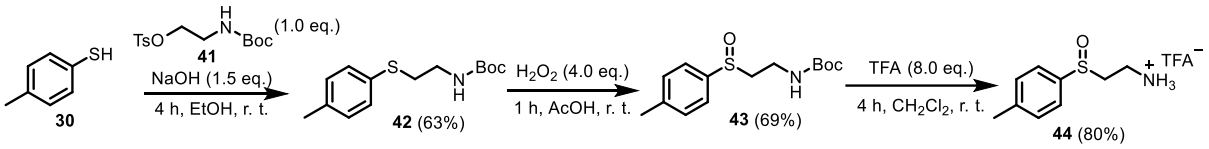

Figure 22: Synthesis of **44** from **30** as a cascade of amine addition, sulfide oxidation and amine deprotection.

3.2 Kinetic resolution of sulfoxides

Previously developed conditions for enzymatic kinetic resolution had been used as a standard procedure for substrates **29, 31, 37** and **40**.[55] Given the cysteine-based catalytic activity of MsrA, DTT had been chosen as a reducing agent, while phosphate buffer maintained stability of the enzyme. Both solutions of DTT and phosphate buffers were prepared fresh. Substrates were added as solutions in acetonitrile.

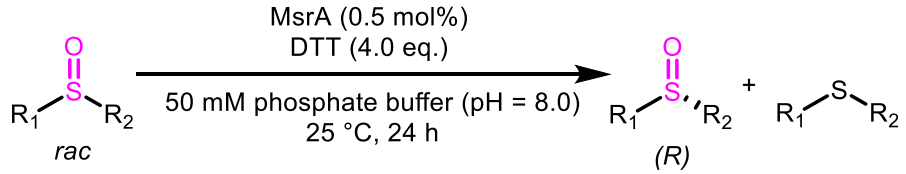

Figure 23: Chemoenzymatic deracemization of substrates **32, 34, 40** and **44** with MsrA.

*Due to capacity limitations of HPLC machine, only part of the crude product had been purified. The yield had been extrapolated for the entire mixture.

After 24 hours, reaction mixtures were extracted and analysed using HPLC-UV/Vis. Substrates with visible conversion were subsequently subjected to chiral HPLC to determine the ee of the reaction.

Table 3: Summary of kinetic resolution of **32, 34, 40** and **44**; n. d. = not determined.

Substrate	Conversion [%] (WT)	WT ee [%]	Conversion [%] (F52L)	F52L ee [%]
32	<1	<1	6	4
34	<1	<1	4	<3
40	Decomposed	n. d.	Decomposed	n. d.
44	<1	n. d.	<1	n. d.

Sadly, as *Table 3* suggests, none of the substrates demonstrated significant activity both with WT and F52L. A number of things could be derived from this information. Firstly, as our previous work discussed, smaller aliphatic chains (including butyl moiety) underwent total conversion with the mutant variant (F52L).[55] It can be reasoned that the cavity of the enzyme can no longer accommodate larger alkyl chains (as demonstrated by the rapid decrease in reactivity). These findings can be further reinforced by molecular dockings of known unreactive compounds into wtMsrA active site (Figure 26). Surprisingly, sulfoxide **44** showed almost no reaction – despite its hydroxyl analogue **45** demonstrating high reactivity. This fact can be justified by the positive charge on the nitrogen atom that is repelled by the hydrophobic cavity of F52, W53 (WT) and L52, W53 (F52L).

Additionally, HPLC analysis of **37** showed decomposition of the product. It turned out that the reaction conditions, namely buffer and DTT were responsible. Due to the established nature of condition protocol, no changes were made to the procedure. Furthermore, storage of **37** proved to be difficult with regards to its high instability, effectively rendering **37** unviable for the resolution.

Despite none of the substrates mentioned above having demonstrated sufficient reactivity, one entry from another screening in our lab showed significant conversion. Sulfoxide **45** proved to be an honest candidate for future study as it had not reacted with WT but was specific to F52L. It can be theorized that Leu-52 is responsible for the reactivity, though exact mechanism remains unclear (Figure 25).

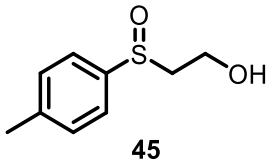

45

Figure 24: Structure of sulfoxide **45**.

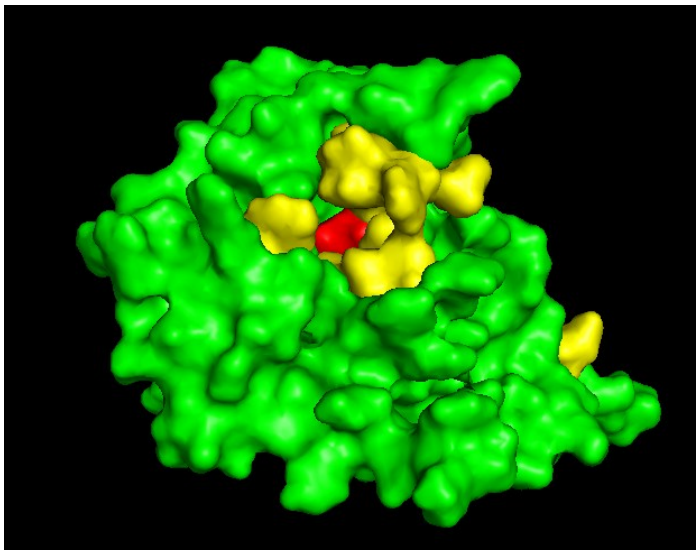

Figure 25: 3D structure of MsrA along with its enzymatic cavity (yellow) and F52L mutation (red).

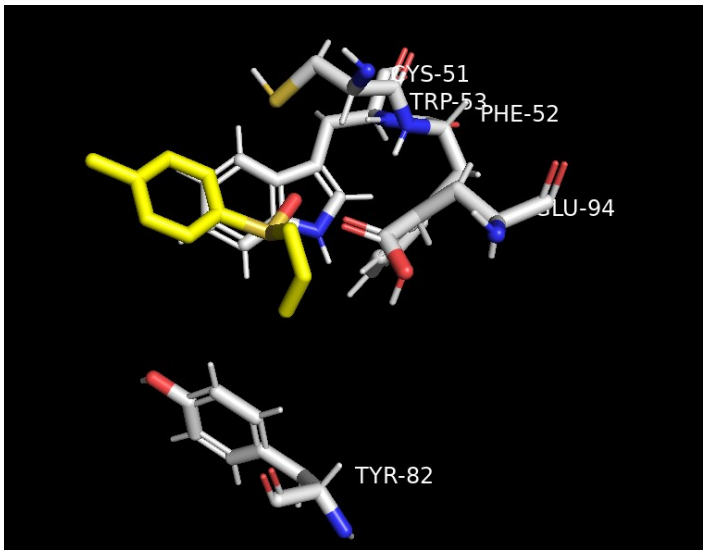

Figure 26: Molecular docking of (S)-1-propyl-4-(methylsulfinyl)benzene (yellow) in the enzymatic cavity of WT MsrA, with the key aminoacids C51, F52, W53, Y84 and E94 shown. It is clear that the substrate does not fit into the enzymatic cavity, suggesting the same mechanism for bulkier groups in the modified variant F52L.

3.3 Development of a novel general method for asymmetric synthesis of sulfoxides

In our previous work, it has been revealed that the benzoxazole moiety in sulfoxide **46** serves as a better leaving group (Figure 27) with a pKa of 24, slightly lower than that of chloromethyl.[56] However, little research has been done on preparing an optically pure version of sulfoxide **46**. If successful, it would suggest new ways of synthesizing optically active sulfoxides. We therefore devised a strategy on how to effectively synthesize sulfoxide **46** in its optically active form.

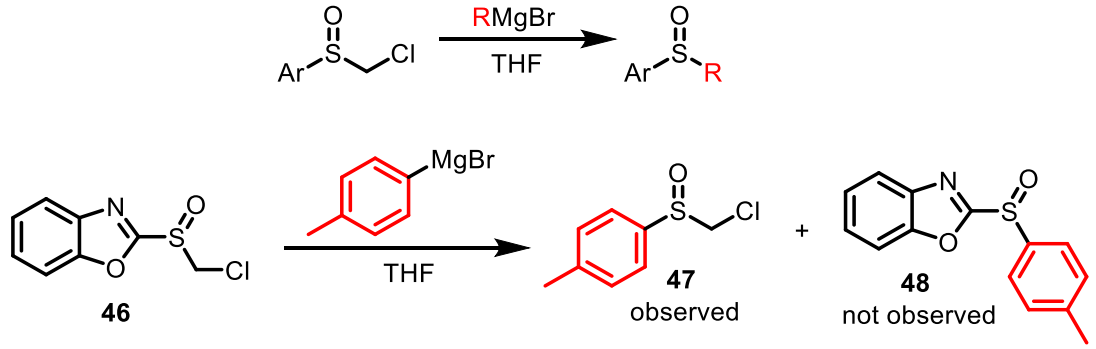

Figure 27: Benzoxazole moiety serves as a complementary group to chloromethyl moiety when screened for regioselective Grignard substitution.

In accordance with previous experiments in our laboratory, the approach of subjecting a racemic mixture to enzymatic resolution to produce the desired product was deemed reasonable. Previous experiments concluded that DmsABC is reactive with **46** but is unviable for large scale synthesis due to cytotoxic effects and limited solubility. Unfortunately, both WT and F52L MsrA turned out to be unreactive with **46**. Consequently, a new asymmetric method for the synthesis of **(*S*)-46** has been investigated.

We envisaged the synthesis of **(*S*)-46** by alfa-chlorination of **(*R*)-49** (Figure 28), a product of enzymatic resolution of **49,** which demonstrated favourable results with MsrA.

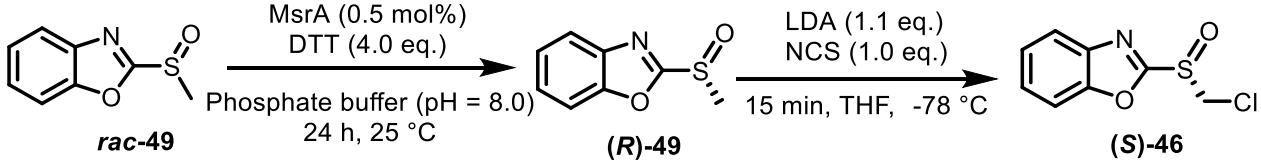

Figure 28: Proposed synthesis of **(*S*)-46** by alfa-chlorination of optically pure **(*R*)-49**. In the initial stage, ***rac*-49** was selected for alfa-chlorination instead.

This approach unfortunately yielded poor results, with **46** either yielding a complex mixture or not being visible in the reaction mixture at all. After further analysis, it was determined that the deprotonated intermediate of **49** was itself unstable and prone to decomposition.

With alfa-chlorination methods having turned out to be unviable, attention was given to selective oxidation of sulfide **50**. Conventional asymmetric oxidation methods such as the Kagan or Modena procedure (Figure 29) were applied, though attempts resulted in complex mixtures with minimal yields of the desired product **(*S*)-46**.

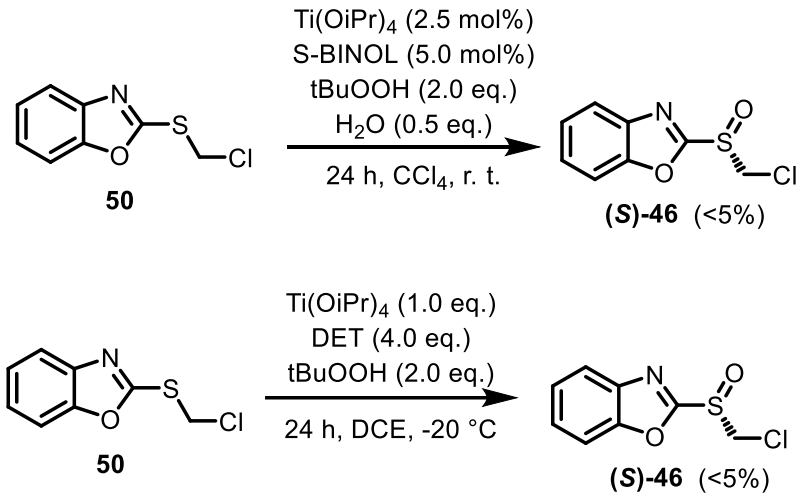

Figure 29: Kagan (top) and Modena (bottom) procedures, applied in synthesis of **(*S*)-46**.

Poor susceptibility of **50** to oxidation could be attributed to the relative acidity of the benzoxazole moiety, coupled with the negative induction effect of chloromethyl group, effectively drawing electron density away from the sulfur atom. Interestingly, a recently developed ligand-stabilized manganese catalyst has been shown to provide a wide range of

products, including **(*S*)-49**.[34] We therefore synthesized the ligand before attempting to study the effects of the catalyst on preparation of **(*S*)-46** (Figure 30).

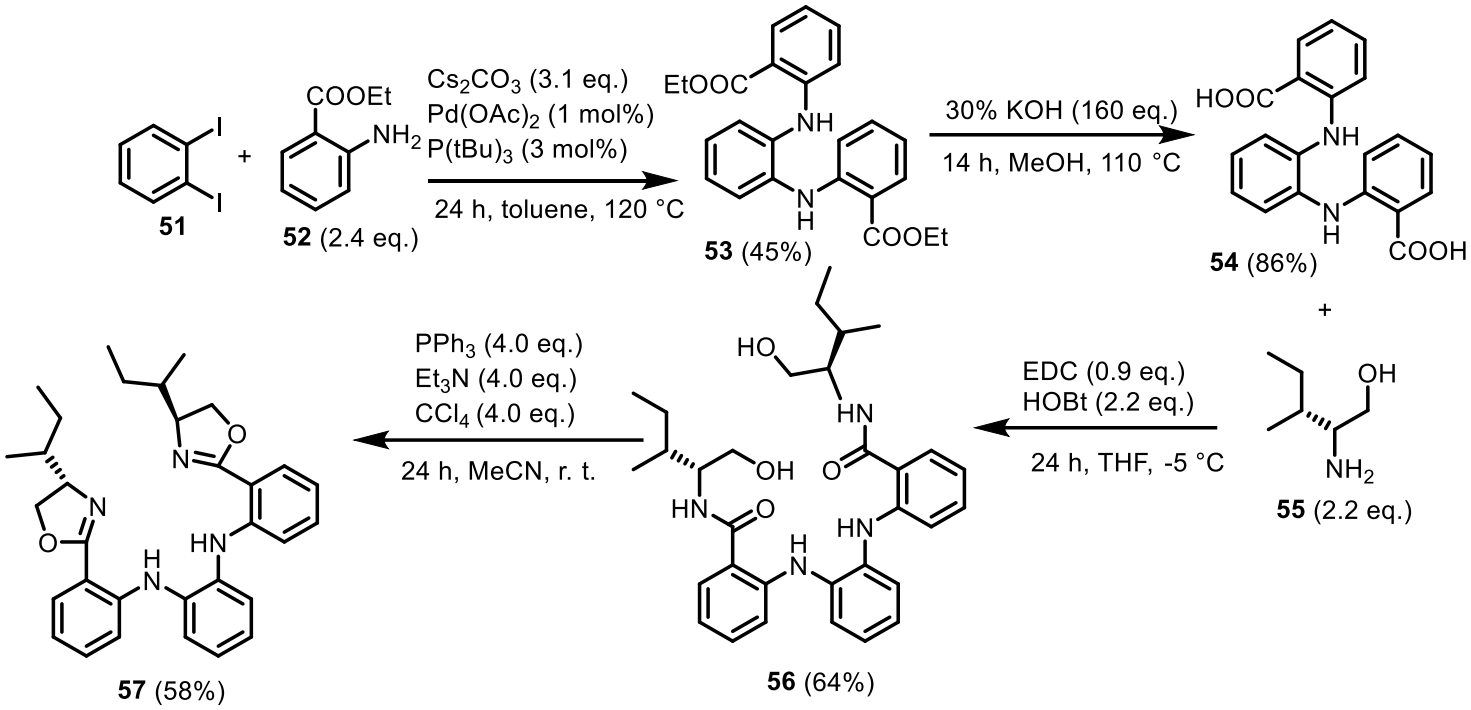

Figure 30: Schematic representation of synthesis of ligand **57**.

Synthesis of **57** had been done by modifying a previous reported procedure.[57] Intermediate **53** was obtained in modest yield of 45% compared to 39% in the reported protocol. After a 24h reflux, **51** was still visible in the reaction mixture, indicating a partial conversion. Optimisation of the reaction had not been performed, though stoichiometry of the reactants and reaction time could have yielded better results. Basic hydrolysis of **53** yielded **54** in 85% yield. Due to poor solubility in the mobile phase, dry loading technique had to be implemented when purifying **54**. Reaction with amine **55** yielded compound **56** in 64% yield, though crude **56** proved to be difficult to purify. In the final step, cyclization of amine 56 gave product **57** in 58%.

The ligand **57** was then tested for asymmetric chemical oxidation of sulfide **50** (Figure 31). Unfortunately, the reported condition provided no conversion of the starting material. Also, increase of catalyst loading and reaction conditions (temperature, time) has not led to conversion improvements (*Table 4*). Poor reactivity of **50** could be attributed to its electron-withdrawing nature as discussed above. This theory was further reinforced with oxidation attempts without the catalyst in the presence of hydrogen peroxide (<5% conversion) and mCPBA (20 % conversion).

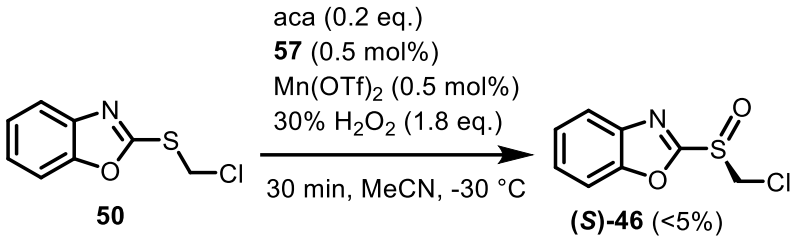

Figure 31: Asymmetric oxidation of **50** to **(*S*)-46**.

Table 4: Reaction parameters of asymmetric oxidation of **(*S*)-46**. Increased presence of catalyst, nor the oxidant resulted in a favourable conversion.

Entry	**57** [eq.]	$Mn(OTf)_2$ [eq.]	30% H_2O_2 [eq.]	Temperature [°C]	Reaction time	Conversion
1	0.005	0.005	1.8	-30 °C gradually to r. t.	24 h	<5%
2	0.035	0.035	3.6	-30 °C gradually to r. t.	24 h	<5%

The original reasoning behind synthesis of **(*S*)-46** lied in having a molecule with two distinct side chains that differed in pKa as to enable regioselective substitution (Figure 32). As a wide range of methods were applied on synthesizing **(*S*)-46** with no result, different molecules meeting criteria in Figure 32 were devised. Focus was also given to preserving properties that would allow for in-vitro (water solubility) or in vivo (minimal cytotoxicity) oxidations.

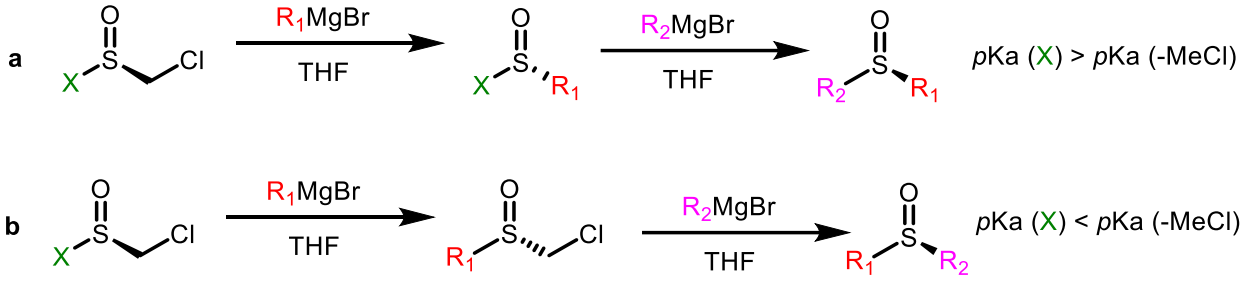

Figure 32: Regioselective substitution of chloromethyl group when subjected to Grignard reagents.

Based on these criteria, several substrates containing and alkynyl moiety have previously been devised but suffered with several problems, namely poor solubility, insufficient Grignard regioselectivity and instability. Consequently, compound **58** has been theorized, serving as a blueprint for future study.

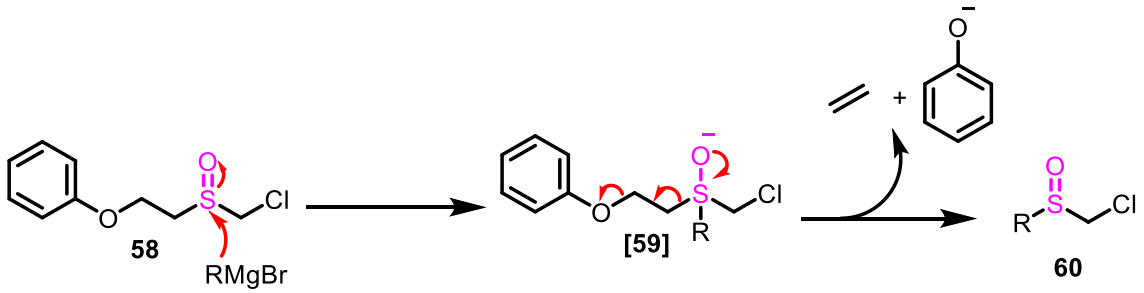

Figure 34: Structure of **25** along with its 1,2-elimination mechanism when subjected to a strong nucleophile.

4 Experimental section

4.1 General procedure

If not mentioned otherwise, all starting reagents and materials were commercially available with purity of <95 % and used without further treatment. Anhydrous THF was obtained via distillation with sodium/benzophenone under nitrogen atmosphere. Other anhydrous solvents were prepared by drying over 4 Å molecular sieves. Argon was utilized as an inert atmosphere for reaction mixtures. pH indication was performed with Lach-Ner indication papers. Analytical TLC was performed with 60 Å 0,2 mm F_{254} plates, with visualization done by UV (λ = 254 nm, λ = 356 nm) light, followed by conventional staining methods (Vanillin, Ellman's reagent and iodine vapours). 60 Å silica gel (0,063 – 0,2 mm) was used for column chromatography along with basic alumina (0,048 – 0,2 mm). ^{1}H NMR spectra were measured from Bruker AVANCE III 600 at 400 MHz, while ^{13}C NMR spectra at 101 MHz and ^{1}H decoupled. Chemical shifts (δ) are given in ppm relative to either residual or internal solvent peak; $(CD_3)_2SO$: δ(H) = 2,50; δ(C) = 39,5; $CDCl_3$: δ(H) = 7,26; δ(C) = 77,2. Coupling constants J are given in Hz, with multiplicity given as s for singlet, d for doublet, t for triplet, q for quadruplet and m for multiplet. Enantiomeric excess (ee) was measured using SPD-M20A detector on Daicel Chiralpak® IA column as a stationary phase. Detailed conditions are given for each substrate. Absolute configurations were determined in accordance with previous literature.[53–55] HRMS data was obtained with ESI on Agilent 6530 Q-TOF MS or Q-TOP COMPACT Bruker spectrometer. UV-Vis absorption spectra were measured on BioDrop Touch spectrometer. Analytical HPLC was used under following conditions: Agilent Eclipse plus C18 column (3.5 µL, 4.6×100 mm); UV/Vis detection at λ_{obs} = 254 nm; flow rate 0.4 mL/min; and gradient elution method (0.1% formic acid – CH_3CN from 95:5 to 0:100 in 16 min). Infrared spectra (IR) were obtained with Nicolet Avatar 370 FT-IR ATR (thin film), absorptions are given in cm^{-1}. Preparative HPLC was performed under following conditions: Agilent ZORBAX SBC18 column (5 µL, 9.4×150 mm); UV/Vis detection at λobs = 254 nm; flow rate 4 mL/min; gradient elution method (0.1% aqueous trifluoroacetic acid – CH3CN from 95:5 to 0:100 in 20 min.

4.2 Synthesis of *p*-tolyl sulfoxides

1-methyl-4-(pentylsulfinyl)benzene (32)

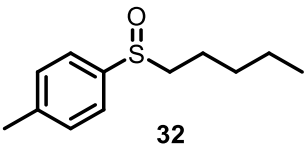

32

Compound **32** was prepared by a modified reported procedure.[53] 200 mg (1.6 mmol) of 4-methylbenzenethiol **30** was displaced into a 50 ml flask along with 96 mg (2.4 mmol) of NaOH and 6 ml EtOH. After 5 minutes of stirring at room temperature, 391 mg (2.4 mmol) of 1-bromopentane was added dropwise. The reaction progress was monitored by TLC analysis, utilizing CH_2Cl_2/cyclohexane (1:5) as a mobile phase and UV light and Ellmann's reagent (0,1% DTNB in 1 : 1 mixture of TRIS buffer and EtOH) as visualization techniques. The reaction mixture was stirred at room temperature for 5.5 hours before being quenched with saturated solution of NH_4Cl (10 ml). After quenching, the reaction mixture was extracted with EtOAc (3 × 15 ml), the organic phase washed with brine, dried over $MgSO_4$ and concentrated in vacuo to give a faint yellow oil **31** (368 mg) which was forwarded to the next step without further purification.

76 mg (0.4 mmol) of **31** was subsequently dissolved in 2 ml glacial acetic acid and 164 µl (1,6 mmol) of concentrated hydrogen peroxide (30%) was added dropwise. The reaction progress was monitored by TLC analysis, utilizing cychlohexane/EtOAc (5:1) as a mobile phase and UV light as a visualization technique. After 1 hour at room temperature, the reaction mixture was quenched by adding 2M NaOH solution, extracted with CH_2Cl_2 (3 × 20 ml), the organic phase washed with brine, dried over $MgSO_4$ and concentrated in vacuo. Crude product was purified with column chromatography (silica, cyclohexane/EtOAc 5 : 1) to give **32** as a colourless oil (61 mg, 82%). **^{1}H NMR** (400 MHz, $CDCl_3$) δ 7.50 (d, J = 8.0 Hz, 2H), 7.31 (d, J = 7.9 Hz, 2H), 2.83 – 2.67 (m, 2H), 2.41 (s, 3H), 1.79 – 1.55 (m, 2H), 1.35 (m, 4H), 0.87 (t, J = 7.0 Hz, 3H). ; **^{13}C NMR** (101 MHz, $CDCl_3$) δ 141.5, 141.0, 130.0, 124.2, 57.5, 30.9, 22.4, 22.0, 21.5, 13.9. **IR** (ν_{max}/cm^{-1}) 3458, 3049, 2954, 2925, 2858, 1495, 1088, 1038. **HRMS** (ESI): *m/z* $[M+H]^+$ calculated for $C_{12}H_{18}OS$: 211.1157, found: 211.1300. The acquired IR and ^{1}H spectra were in agreement with reported literature.[58]

1-methyl-4-(hexylsulfinyl)benzene (34)

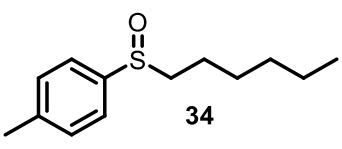

34

Compound **34** was prepared by modified reported procedure.[53] 200 mg (1.6 mmol) of **30** was displaced in a 50 ml flask along with 96 mg (2.4 mmol) of NaOH and 6 ml EtOH. After stirring for 5 min at room temperature, 365 mg (2.4 mmol) of 1-bromohexane was added and the mixture left to stir

at room temperature for 4 hours. The reaction progress was monitored by TLC analysis, utilizing CH_2Cl_2/cyclohexane (1:5) as a mobile phase and UV light and Ellman's reagent (details in preparation of **32**) as visualization techniques. After 4 hours, the reaction mixture was quenched using saturated solution of NH_4Cl, extracted with EtOAc (2 × 15 ml) and brine, dried over $MgSO_4$ and concentrated in vacuo to give **33** as a yellowish oil (272 mg) which was forwarded to the next step without purification.

102 mg (0.51 mmol) of **33** was subsequently dissolved in 4 ml glacial acetic acid and 207 µl (2.0 mmol) of concentrated hydrogen peroxide (30%) was added dropwise. The reaction mixture was left to stir at room temperature for 1 hour. The reaction progress was monitored by TLC analysis, utilizing cychlohexane/EtOAc (5:1) as a mobile phase and UV light as a visualization technique. After 1 hour at room temperature, the reaction mixture was quenched using 2M NaOH solution, extracted with CH_2Cl_2 (3 × 20 ml), the organic phase washed with brine, dried over $MgSO_4$ and concentrated in vacuo. Crude product was subjected to column chromatography (silica, cyclohexane/EtOAC 5 : 1) to give **34** as a colourless oil (88 mg, 77%). **^{1}H NMR** (400 MHz, $CDCl_3$) δ 7.49 (d, J = 8.1 Hz, 2H), 7.30 (d, J = 7.9 Hz, 2H), 2.81 – 2.68 (m, 2H), 2.39 (s, 3H), 1.75 – 1.53 (m, 2H), 1.46 – 1.32 (m, 2H), 1.30 – 1.20 (m, 4H), 0.84 (t, J = 5.6 Hz, 3H). **^{13}C NMR** (101 MHz, $CDCl_3$) δ 141.4, 140.9, 130.0, 124.2, 57.5, 31.4, 28.4, 22.5, 22.3, 21.5, 14.0. **IR** (ν_{max}/cm^{-1}) 3465, 3051, 2956, 2927, 2860, 1495, 1038. **HRMS** (ESI): *m/z* $[M+H]^+$ calculated for $C_{13}H_{20}OS$: 225.1313, found: 225.1429. The acquired ^{1}H, ^{13}C and HRMS spectra were in agreement with reported literature.[59]

triisopropyl((*p*-tolylsulfinyl)ethynyl)silane (37a)

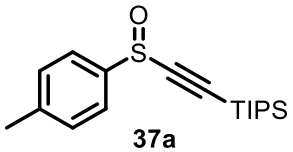

37a

200 mg (1.3 mmol) of **35** along with 5 ml dry THF was displaced into a degassed 50 ml flask. The resulting mixture was cooled to -40 °C (MeCN/dry ice bath) and 199 µl (2.0 mmol) of $SOCl_2$ was added dropwise. After 45 minutes, the solution containing **36** was concentrated in vacuo. In a new degassed Schlenk flask, 321 µl (1.4 mmol) of triisopropylsilylacetylene along with 5 ml dry THF was added. The resulting mixture was cooled to -78 °C (acetone/dry ice bath) and 700 µl (1.4 mmol) of 2M *n*-BuLi was added dropwise. After 10 minutes of stirring, content of the 50 ml flask containing **36** was redissolved in dry THF and added dropwise to the Schlenk flask. After 45 minutes at -78 °C, the reaction mixture was quenched with saturated NH_4Cl solution, extracted with EtOAc (2 × 30 ml), the organic phase washed with brine, dried over $MgSO_4$ and concentrated in vacuo. The crude brown product (194 mg) was subjected to column

chromatography (silica, cyclohexane/EtOAc 5 : 1) to give **37a** as a lightly coloured oil (86 mg, 21%). **^{1}H NMR** (400 MHz, $CDCl_3$) δ 7.72 (d, J = 8.3 Hz, 2H), 7.34 (d, J = 8.0 Hz, 2H), 2.43 (s, 3H), 1.07 – 1.03 (m, 21H). **^{13}C NMR** (101 MHz, $CDCl_3$) δ 142.6, 141.3, 130.3, 125.5, 108.3, 102.6, 21.6, 18.6, 11.2. **HRMS** (ESI): *m/z* $[M+H]^+$ calculated for $C_{18}H_{28}OSSi$: 321.1708, found: 321.1741. The acquired spectra were in agreement with reported literature.[60]

methyl 4-methylbenzenesulfinate (38)

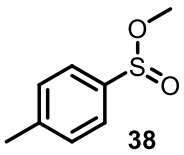

38

300 mg (1.9 mmol) of sodium 4-methylbenzenesulfinate **35** was displaced into a 100 ml flask under argon atmosphere. Next, 7.5 ml of dry THF was added and the mixture cooled down to 0 °C with ice/water bath. Next, 275 µl (3.8 mmol) of $SOCl_2$ was added dropwise. The reaction progress was monitored by TLC analysis, utilizing cyclohexane/EtOAc (2:3) as a mobile phase and UV light as a visualization technique. After 1 hour at 0 °C, 575 µl (14.3 mmol) MeOH and 1.96 ml (14.3 mmol) Et_3N were added. During the addition, fumes of HCl were visible. After 4 hours at 0 °C, the milky reaction mixture was quenched with 15 ml of saturated $NaHCO_3$ solution, extracted with EtOAc, the organic phase washed with brine, dried over $MgSO_4$ and concentrated in vacuo. The crude product (249 mg) was subjected to column chromatography (silica, cyclohexane/EtOAc 3 :1) to afford **38** as a colourless oil (196 mg, 61%).**^{1}H NMR** (400 MHz, $CDCl_3$) δ 7.58 (d, J = 9.0 Hz, 2H), 7.33 (d, J = 9.5 Hz, 2H), 3.46 (s, 3H), 2.42 (s, 3H).**^{13}C NMR** (101 MHz, $CDCl_3$) δ 143.0, 141.1, 129.9, 125.5, 49.5, 21.6. The acquired spectra were in agreement with reported literature.[61]

trimethyl((*p*-tolylsulfinyl)ethynyl)silane (37c)

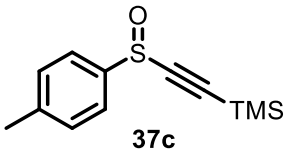

37c

232 µl (1.7 mmol) of ethynyltrimethylsilane along with 10 ml of dry toluene was displaced in a Schlenk flask under argon atmosphere. Next, the reaction mixture was cooled to -78 °C (dry ice/acetone bath) and 840 µl (1.7 mmol) of *n*-BuLi (2M in THF) was added dropwise. After 15 minutes of stirring, 261 mg (1.5 mmol) of **38** in dry toluene was added dropwise to the reaction mixture and left to stir for 1 hour at -78 °C. Throughout the reaction, the colour changed from light yellow to dark orange. The reaction progress was monitored by TLC analysis, utilizing cyclohexane/EtOAc (5:1) as a mobile phase and UV light as a visualization technique. After 1 hour at -78 °C, the reaction mixture was quenched with saturated NH_4Cl solution, extracted with EtOAc (3 × 20 ml), the organic phase washed with brine, dried over $MgSO_4$ and

concentrated in vacuo. Brown crude product (245 mg) was subjected to column chromatography (silica, cyclohexane/EtOAc 5 : 1) to give **37c** as a faint yellow oil (97 mg, 27%).**^{1}H NMR** (400 MHz, $CDCl_3$) δ 7.72 (d, J = 8.2 Hz, 2H), 7.37 (d, J = 7.9 Hz, 2H), 2.44 (s, 3H), 1.25 (s, 9H).**^{13}C NMR** (101 MHz, $CDCl_3$) δ 143.1, 140.2, 130.5, 125.4, 90.2, 82.0, 49.6, 21.7. **HRMS** (ESI): *m/z* $[M+H]^+$ calculated for $C_{12}H_{16}OSSi$: 237.0764, found: 237.0752.

1-(ethynylsulfinyl)-4-methylbenzene (40)

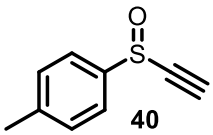

40

35 mg (0.15 mmol) of **37c** was displaced into a 50 ml flask and dissolved in 4.5 ml 96 % EtOH. The reaction mixture was cooled to 0 °C (ice/water bath) and 42 mg (1.2 mmol) of KF was added dropwise as a 0.5 ml solution of EtOH/water 1 : 1. The reaction progress was monitored by TLC analysis, utilizing cyclohexane/EtOAc (3:2) as a mobile phase and UV light as a visualization technique. After 4 hours at 0 °C, the reaction mixture was quenched with 15 ml of water, extracted with EtOAc (2 × 20 ml), the organic phase washed with brine, dried over $MgSO_4$ and concentrated in vacuo. Crude product was subjected to column chromatography (silica, cyclohexane/EtOAc 3 : 2) which yielded **40** as a lightly coloured oil (22 mg, 92%).**^{1}H NMR** (400 MHz, $CDCl_3$) δ 7.71 (d, J = 8.3 Hz, 2H), 7.36 (d, J = 8.2 Hz, 2H), 3.70 (s, 1H), 2.43 (s, 3H).**^{13}C NMR** (101 MHz, $CDCl_3$) δ 143.1, 140.2, 130.5, 125.3, 90.2, 82.0, 21.6. **IR** (ν_{max}/cm^{-1}) 3192, 3053, 2941, 2871, 2036, 1595, 1493, 1128, 1086. **HRMS** (ESI): *m/z* $[M+H]^+$ calculated for C_9H_8OS: 165.0369, found: 165.0360. The acquired spectra were in agreement with reported literature.[60]

tert-butyl ((*p*-tolylthio)methyl)carbamate (42)

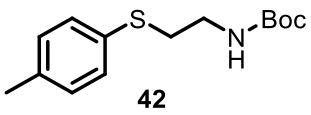

42

700 mg (2.2 mmol) of tert-butyl (2-tosylethyl)carbamate **41** along with 275 mg (2.2 mmol) of **30** and 133 mg (3.3 mmol) of NaOH were displaced in a 100 ml flask. Next, 10 ml of 96% EtOH was added and the reaction mixture left to stir at room temperature for 4 hours. The reaction progress was monitored by TLC analysis, utilizing cyclohexane/EtOAc (9:1) as a mobile phase and UV light as a visualization technique. After 4 hours at room temperature, the reaction mixture was quenched with saturated NH_4Cl solution, extracted with EtOAc (2 × 50 ml), the organic phase washed with brine, dried over $MgSO_4$ and concentrated in vacuo. The crude yellow oil (651 mg) was subjected to column chromatography (silica, cyclohexane/EtOAc 9 : 1) to give **42** as a colourless oil (371 mg, 63%).**^{1}H NMR** (400 MHz, $CDCl_3$) δ 7.28 (d, J = 8.0, 1.4 Hz, 2H), 7.10 (d, J = 7.8 Hz, 2H), 4.91 (s, 1H), 3.29 (t, J = 6.3 Hz, 2H), 2.98 (t, J = 6.4 Hz, 2H), 2.32 (s,

3H), 1.43 (s, 9H).**^{13}C NMR** (101 MHz, $CDCl_3$) δ 155.8, 136.9, 131.4, 130.9, 130.0, 79.5, 39.7, 35.1, 28.5, 21.1. The acquired spectra were in agreement with previous literature.[62]

tert-butyl ((*p*-tolylsulfinyl)methyl)carbamate (43)

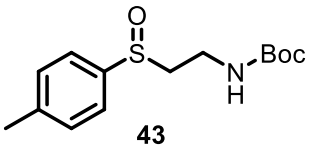

43

371 mg (1.4 mmol) of **42** along with 10 ml of glacial acetic acid was displaced in a 100 ml flask. Next, 568 µl (5.6 mmol) of concentrated hydrogen peroxide (30%) was added dropwise and the reaction mixture left to stir at room temperature for 1 hour at room temperature. Reaction progress was monitored by TLC analysis, utilizing cyclohexane/EtOAc (2:3) as a mobile phase and UV light as a visualization technique. After 1 hour at room temperature, the reaction mixture was quenched with 10 % NaOH solution, extracted with EtOAc (2 × 50 ml), the organic phase washed with brine, dried over $MgSO_4$ and concentrated in vacuo. The crude product (312 mg) was subjected to column chromatography (silica, cyclohexane/EtOAc 1 : 3) to give **43** as a colourless oil (258 mg, 69%).**^{1}H NMR** (400 MHz, $CDCl_3$) δ 7.50 (d, J = 8.0 Hz, 2H), 7.34 (d, J = 7.9 Hz, 2H), 5.19 (s, 1H), 3.63 – 3.45 (m, 2H), 3.11 (m, 1H), 2.84 (dt, J = 13.5, 5.5 Hz, 1H), 2.42 (s, 3H), 1.42 (s, 9H).**^{13}C NMR** (101 MHz, $CDCl_3$) δ 156.0, 141.8, 140.0, 130.3, 124.1, 79.9, 35.1, 28.5, 21.6. The acquired spectra were in agreement with previous literature.[63]

2-(*p*-tolylsulfinyl)ethan-1-amine (44)

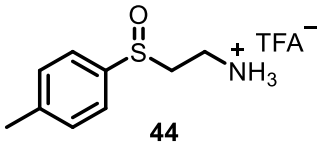

44

238 mg (0.84 mmol) of **43** along with 10 ml of CH_2Cl_2 was displaced into a 100 ml flask. Next, 1.03 ml (13.4 mmol) of trifluoroacetic acid (TFA) was added dropwise and the reaction mixture left to stir at room temperature for 5 hours. Reaction progress was monitored by TLC analysis, utilizing CH_2Cl_2/MeOH (9:1) as a mobile phase and UV light as a visualization technique. After 5 hours at room temperature, the reaction mixture was concentrated in vacuo and one tenth of the crude product was purified via HPLC (t_r = 6.9 min) to give TFA salt of **44** as an orange solid (12 mg, 80%).**^{1}H NMR** (400 MHz, DMSO) δ 7.92 (s, 2H), 7.57 (d, J = 9 Hz, 2H), 7.44 (d, J = 8.0 Hz, 2H), 3.29 – 3.23 (m, 1H), 3.16 – 3.10 (m, 1H), 3.04 – 2.96 (m, 1H), 2.94 – 2.87 (m, 1H), 2.39 (s, 3H).**^{13}C NMR** (101 MHz, DMSO) δ 141.2, 139.7, 130.0, 124.0, 52.0, 32.9, 20.9.**^{19}F NMR** (376 MHz, DMSO) δ -73.5. **IR** (ν_{max}/cm^{-1}) 3400, 3141, 2920, 2625, 1716, 1601, 1431, 1124, 1038, 937, 798, 719, 505. **HRMS** (ESI): *m/z* $[M+H]^+$ calculated for

$C_9H_{13}NOS$: 184.0791, found: 184.0787. The acquired ^1H spectra were in agreement with reported literature.[64]

4.3 General procedure for kinetic resolution of sulfoxides with MsrA

MsrA variants were prepared according to a general procedure reported by our laboratory.[55] The final concentration of the enzyme was determined from absorbance at UV light using a known extinction coefficient (typically ~20 mg/ml). As a result, volumes of enzyme solutions displaced into resolution reactions varied (amounting to 0.5 mol%).

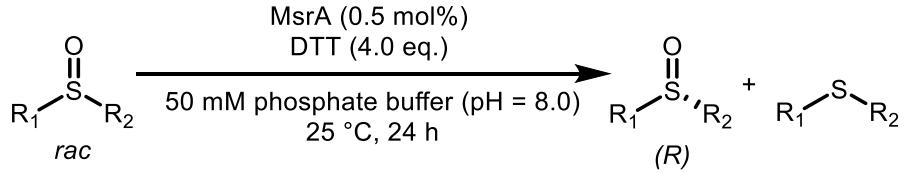

Each 1.5 ml Eppendorf tube contained precisely 500 µl of reaction mixture containing 250 µl of 50mM DTT (4.0 eq.) in phosphate buffer (50 mM Na_2HPO_4/NaH_2PO_4, pH = 8.0), 10 µl of 324 mM (1.0 eq.) racemic sulfoxide in MeCN and corresponding amount of 0.5 mol% MsrA and phosphate buffer. Due to different concentrations of isolated enzymes, the displaced amount of both enzyme and buffer solutions differed – general procedure listed below accounts for WT MsrA with a concentration of 24 mg/ml and F52L MsrA with a concentration of 15 mg/ml.

WT: 224 µl of phosphate buffer was displaced into a 1.5 ml Eppendorf tube, followed by 250 µl of 50mM DTT in phosphate buffer and 10 µl 324mM (3.2 µmol) racemic sulfoxide in MeCN/phosphate buffer 1 : 1. Next, 16 µl (0.016 µmol) of WT MsrA in Tris buffer (50 mM Tris-HCl, pH = 8.0) was added and the reaction mixture incubated for 24 hours at 25 °C. Conversion had been monitored by analytical HPLC. After 24 hours, the reaction mixture was extracted with 5 ml EtOAc, the organic phase washed with brine, dried over $MgSO_4$ and concentrated in vacuo. Enantiomeric excess of the isolated product was determined by HPLC with chiral stationary phase.

F52L: 214 µl of phosphate buffer was displaced into a 1.5 ml Eppendorf tube, followed by 250 µl of 50mM DTT in phosphate buffer and 10 µl 324mM (3.2 µmol) racemic sulfoxide in MeCN/phosphate buffer 1 : 1. Next, 26 µl (0.016 µmol) of WT MsrA in Tris buffer (50 mM Tris-HCl, pH = 8.0) was added and the reaction mixture incubated for 24 hours at 25 °C. Conversion had been monitored by HPLC. After 24 hours, the reaction mixture was extracted

with 5 ml EtOAc, the organic phase washed with brine, dried over $MgSO_4$ and concentrated in vacuo. Enantiomeric excess of the isolated product was determined by HPLC with chiral stationary phase.

(R)-1-methyl-4-(pentylsulfinyl)benzene (32)

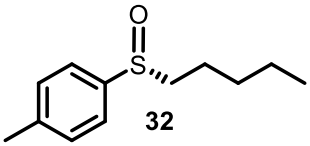

32

wt MsrA: conversion <1 %, ee < 1 %, **F52L**: conversion = 6 %, ee = 4 % . Enantiomeric excess was determined by HPLC (IA chiralpak®: heptane/isopropanol (95 : 5), flow rate 1 ml/min; 25 °C; 254 nm; 20 min, t_r = 12.9 min, 14.4 min

(R)-1-methyl-4-(hexylsulfinyl)benzene (34)

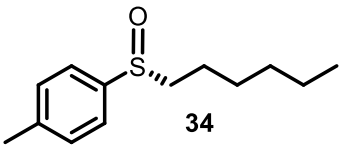

34

wt MsrA: conversion <1 %, ee < 1 %, **F52L**: conversion = 4 %, ee = <3 % . Enantiomeric excess was determined by HPLC (IA chiralpak®: heptane/isopropanol (95 : 5), flow rate 1 ml/min; 25 °C; 254 nm; 20 min, t_r = 12.1 min, 13.4 min

(R)-2-(*p*-tolylsulfinyl)ethan-1-amine (44)

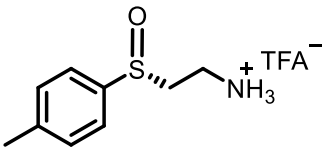

44

wt MsrA: conversion <1 %, ee not determined **F52L**: conversion <1 %, ee not determined.

4.4 Asymmetric oxidation of benzoxazole-containing sulfoxides

2-(methylsulfinyl)benzo[d]oxazole (49)

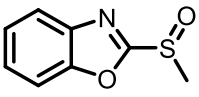

49

300 mg (2.0 mmol) of benzo[d]oxazole-2-thiol were displaced into a 100 ml flask along with 15 ml EtOAc. Next, 317 mg (2.5 mmol) of K_2CO_3 was added and the mixture allowed to stir for 5 minutes at room temperature. 136 µl (2.2

mmol) of MeI was then added dropwise and the reaction mixture left to stir at room temperature for 1 hour. Reaction progress was monitored by TLC analysis, utilizing cyclohexane/EtOAc (4:1) as a mobile phase and UV light and Ellman's reagent as visualization techniques. After 4 hours at room temperature, the milk brown mixture was quenched with water, extracted with EtOAc (2 × 30 ml), the organic phase washed with brine, dried over $MgSO_4$ and concentrated in vacuo to give 2-(methylthio)benzo[d]oxazole as a brown oil (300 mg) which was forwarded to next step without further purification.**^{1}H NMR** (400 MHz, $CDCl_3$) δ 7.68 – 7.64 (dd, J = 9 Hz, 1H), 7.48 (dd, *J* = 7.7, 1.5 Hz, 1H), 7.35 – 7.26 (m, 2H), 2.81 (s, 3H).**^{13}C NMR** (101 MHz, $CDCl_3$) δ 165.9, 152.1, 142.1, 124.4, 124.0, 118.4, 110.0, 14.7. **LRMS** (ESI): *m/z* $[M+H]^+$ calculated for C_8H_7NOS: 166.03, found: 166.10. The acquired ^{1}H and ^{13}C spectra were in agreement with reported literature.[65]

275 mg (1.4 mmol) of 2-(methylthio)benzo[d]oxazole was displaced into a 100 ml flask along with 10 ml of CH_2Cl_2. Next, 340 mg (1.52 mmol) of *m*CPBA (77%) was added and the reaction mixture left to stir at 0 °C (ice/water bath) for 2 hours. Reaction progress was monitored by TLC analysis, utilizing cyclohexane/EtOAc (4:1) as a mobile phase and UV light as a visualization technique. After 2 hours at 0 °C, the reaction mixture was quenched with saturated solution of $NaHCO_3$, extracted with CH_2Cl_2 (3 × 20 ml), the organic phase washed with brine, dried over $MgSO_4$ and concentrated in vacuo. Crude product was subjected to column chromatography (basic alumina, 100% CH_2Cl_2) to give **49** as beige oil (183 mg, 73%).**^{1}H NMR** (400 MHz, $CDCl_3$) δ 7.83 (dd, J = 9 Hz, 1H), 7.66 (d, J = 9.5 Hz, 1H), 7.52 – 7.42 (m, 2H), 3.21 (s, 3H).**^{13}C NMR** (101 MHz, $CDCl_3$) δ 165.0, 152.0, 140.6, 127.3, 125.8, 121.5, 111.7, 40.1. The acquired spectra were in agreement with reported literature.[34]

diethyl 2,2'-(1,2-phenylenebis(azanediyl))dibenzoate (53)

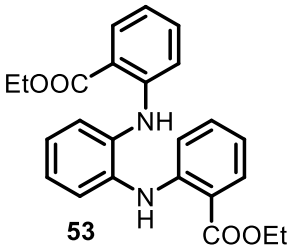

53

Compound **53** was prepared by a modified reported procedure.[57] A Schlenk flask was equipped with 17 mg (0.060 mmol) of $Pd(OAc)_2$ along with 5 ml dry toluene under argon atmosphere. Next, 3.76 mg (0.018 mol) of P(*t*Bu)$_3$ was added and the mixture allowed to stir for 15 min at room temperature. Consequently, 200 mg (0.76 mmol) of **51** and 303 mg (1.8 mmol) of **52** were added, followed by 772 mg (2.4 mmol) of Cs_2CO_3 under strong argon stream. The resulting mixture was left to stir at 120 °C for 24 hours. Reaction progress was monitored by TLC analysis, utilizing cyclohexane/EtOAc (4:1) as a mobile phase and UV light as a visualization technique. After 24 hours, the orange mixture was quenched

with saturated solution of NH_4Cl, extracted with CH_2Cl_2, the organic phase washed with brine, dried over $MgSO_4$ and concentrated in vacuo. The crude product was subjected to column chromatography (silica, cyclohexane/EtOAc 9 : 1) to give **53** as a crystalline yellow solid (140 mg, 45%).**^{1}H NMR** (400 MHz, $CDCl_3$) δ 9.24 (s, 2H), 7.92 (dd, J = 8.0, 1.7 Hz, 2H), 7.43 (dd, J = 5.9, 3.6 Hz, 2H), 7.25 (td, J = 7.2, 1.6 Hz, 2H), 7.10 (dd, J = 6.0, 3.5 Hz, 2H), 7.06 (dd, J = 8.6, 1.1 Hz, 2H), 6.70 (d, J = 8.1 Hz, 2H), 4.27 (q, J = 7.1 Hz, 4H), 1.33 (t, J = 7.1 Hz, 6H).**^{13}C NMR** (101 MHz, $CDCl_3$) δ 168.25, 147.82, 134.90, 133.87, 131.62, 124.41, 123.89, 117.36, 114.65, 113.12, 60.65, 14.42. **HRMS** (ESI): *m/z* $[M+Na]^+$ calculated for $C_{24}H_{24}N_2O_4$: 427.164, found: 427.162. The acquired spectra were in agreement with reported literature.[57]

2,2'-(1,2-phenylenebis(azanediyl))dibenzoic acid (54)

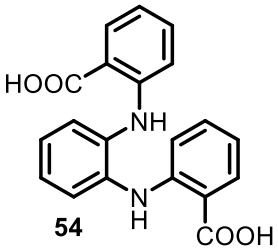

54

Compound **54** was prepared according to reported procedure.[57] 61 mg (0.17 mmol) of **53** was displaced in a 50 ml flask and dissolved in 5 ml MeOH. Next, 1.5 g (27 mmol) of KOH was added as a 30% water solution. The resulting mixture was refluxed for 14 hours. Reaction progress was monitored by TLC analysis, utilizing 100% EtOAc as a mobile phase and UV light as a visualization technique. After 14 hours of refluxing, the dark orange solution was quenched with water and 10 % HCl was added to reduce pH to 4. Next, the mixture was extracted with EtOAc (3 × 20 ml), the organic phase washed with brine, dried over $MgSO_4$ and concentrated in vacuo to give **54** as a crystalline-blood like solid (46 mg, 86 %).**^{1}H NMR** (400 MHz, DMSO) δ 12.92 (s, 2H), 9.58 (s, 2H), 7.84 (dd, J = 8.0, 1.7 Hz, 2H), 7.45 (dd, J = 5.9, 3.6 Hz, 2H), 7.32 (td, J = 8.8, 1.7 Hz, 2H), 7.17 (dd, J = 6.0, 3.5 Hz, 2H), 6.99 (d, J = 8.4 Hz, 2H), 6.73 (t, J = 7.5 Hz, 2H).**^{13}C NMR** (101 MHz , $CDCl_3$) δ 170.6, 147.4, 134.1, 133.9, 131.7, 124.5, 123.4, 117.2, 113.4, 112.4. The acquired spectra were in agreement with reported literature.[57]

N-((2R,3S)-1-hydroxy-3-methylpentan-2-yl)-2-((2-((2-(((2S,3S)-1-hydroxy-3-methylpentan-2-yl)carbamoyl)phenyl)amino)phenyl)amino)benzamide (56)

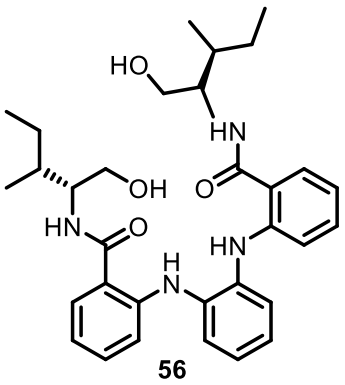

56

Compound **56** was prepared according to reported procedure.[57] 45 mg (0.13 mmol) of **54** in dry THF was displaced in a Schlenk flask. Next, 18 mg (0.12 mmol) of EDC was added, followed by 38 mg (0.28 mmol) of HOBt and 33 mg (0.28 mmol) of **55**. The resulting mixture was cooled to -5 °C (ice/brine + NaCl bath) and stirred for 2 hours under argon atmosphere. Reaction progress was monitored by TLC analysis, utilizing cyclohexane/EtOAc (2:3) as a mobile phase and UV light as a visualization technique. After 2 h at -5 °C, the reaction mixture was left to gradually warm up to room temperature and stir overnight. The dark orange mixture was then concentrated in vacuo and subjected to column chromatography (silica, cyclohexane/EtOAc 2 : 3) to give **56** as a bright yellow oil (45 mg, 64%).**^{1}H NMR** (400 MHz, $CDCl_3$) δ 8.52 (s, 2H), 7.35 (dt, J = 5.8, 3.6 Hz, 4H), 7.15 (t, J = 7.8 Hz, 2H), 7.06 (dd, J = 5.9, 3.5 Hz, 2H), 7.00 (d, J = 8.4 Hz, 2H), 6.70 (t, J = 7.5 Hz, 2H), 6.36 (d, J = 8.5 Hz, 2H), 3.87 (dd, J = 17.8, 8.7 Hz, 4H), 3.75 (dd, J = 11.6, 3.5 Hz, 2H), 3.62 (dd, J = 11.6, 6.0 Hz, 2H), 1.76 – 1.66 (m, 2H), 1.61 – 1.51 (m, 2H), 1.32 – 1.15 (m, 2H), 0.96 (d, J = 6.8 Hz, 6H), 0.91 (t, J = 7.4 Hz, 6H).**^{13}C NMR** (101 MHz, $CDCl_3$) δ 170.4, 145.0, 134.5, 132.1, 127.6, 124.1, 123.1, 119.9, 118.2, 115.1, 63.3, 56.4, 36.0, 25.8, 15.8, 11.5. **HRMS** (ESI): *m/z* $[M+Na]^+$ calculated for $C_{32}H_{42}N_4O_4$: 569.311, found: 569.308. The acquired spectra were in agreement with reported literature.[57]

N1,N2-bis(2-((S)-4-((S)-sec-butyl)-4,5-dihydrooxazol-2-yl)phenyl)benzene-1,2-diamine (57)

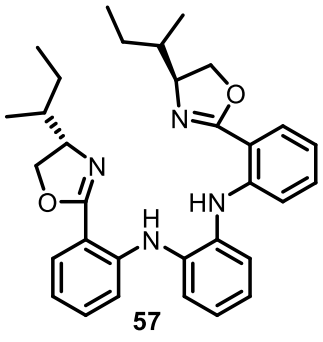

57

Compound **57** was prepared according to reported procedure.[57] 35 mg (0.064 mmol) of **56** dissolved in dry MeCN was displaced in a Schlenk flask. Next, PPh_3 (67 mg, 0.26 mmol), Et_3N (36 µl, 0.2 mmol) and CCl_4 (25 µl, 0.26 mmol) were added. The reaction mixture was left to stir at room temperature for 24 hours. Reaction progress was monitored by TLC analysis, utilizing cyclohexane/CH_2Cl_2 (5:1) as a mobile phase and UV light and Vaniline staining as visualization techniques (**57** appeared as a green spot after heating). After 24 hours at room temperature, the reaction mixture was quenched with water, extracted with CH_2Cl_2 (2 × 20 ml), the organic phase washed with brine, dried over $MgSO_4$ and concentrated in vacuo. The yellow crude

product was subjected to column chromatography (silica, cyclohexane/CH_2Cl_2 5 : 1) to give **57** as a yellow crystalline solid (19 mg, 58%).**^{1}H NMR** (400 MHz, $CDCl_3$) δ 10.46 (s, 2H), 7.75 (dd, J = 8.0, 1.6 Hz, 2H), 7.51 (dd, J = 6.0, 3.5 Hz, 2H), 7.29 – 7.20 (m, 6H), 7.03 (dd, J = 6.0, 3.5 Hz, 2H), 6.72 (t, J = 9.5 Hz, 2H), 4.27 (dd, J = 7.6, 1.5 Hz, 2H), 3.98 (td, J = 8.8, 6.9 Hz, 2H), 1.46 – 1.24 (m, 4H), 0.93 (m 2H), 0.68 (d, J = 6.7 Hz, 6H), 0.59 (t, J = 7.4 Hz, 6H).**^{13}C NMR** (101 MHz, $CDCl_3$) δ 146.0, 135.0, 131.7, 129.9, 123.2, 122.1, 116.9, 113.7, 71.8, 69.0, 39.7, 27.1, 15.0, 10.9. **LRMS** (ESI): *m/z* $[M+H]^+$ calculated for $C_{32}H_{38}N_4O_2$: 511.307, found: 511.305. The acquired spectra were in agreement with reported literature.[57]

General procedure for asymmetric oxidation of sulfides with 57 as a chiral ligand

The general procedure followed protocol from reported literature.[34] 4mM solutions of $Mn(OTf)_2$ (1.96 µmol) and **24** (1.96 µmol) in dry MeCN were displaced in a Schlenk flask and allowed to stir at room temperature for 24 hours. Throughout the reaction, there was a distinct colour change from light yellow to dark orange. After 24 hours, 1-adamantanecarboxylic acid (0.078 mmol) and **17** (0.39 mmol) were added in this order. The turned greenish mixture was cooled to -30 °C (dry ice/MeCN bath) and hydrogen peroxide (0.71 mmol) was quickly added. After 30 minutes, the reaction mixture was quenched with saturated $NaHCO_3$ solution, extracted with CH_2Cl_2, the organic phase washed with brine, dried over $MgSO_4$ and concentrated in vacuo before being purified by column chromatography.

5 Conclusion

In this thesis, several racemic sulfoxides were synthesized and subjected to kinetic resolution using both wild-type and custom-made mutant variant F52L of the enzyme MsrA, probing substrate scope. The results of the resolution demonstrated that pentyl and hexyl chains are too large of a group for the enzyme to tolerate. Same can be said for groups bearing a nitrogen group, with possible redistribution of electron density across the catalytic residues. Certain substrates intended for resolution turned out to be unstable and prone to decomposition, particularly ones containing ethynyl- moiety.

In the second part, several methods have been applied to synthesize optically pure 2-((chloromethyl)sulfinyl)benzo[d]oxazole for its properties in regioselective Grignard additions. Conventional approaches such as Kagan or Modena oxidations were tried out as well as a novel approach utilizing a ligand-stabilized manganese catalyst. Unfortunately, none of these approaches yielded a favourable result. With the substrate's reactivity thoroughly investigated, it can be said that preparation of optically pure 2-((chloromethyl)sulfinyl)benzo[d]oxazole cannot be done using established oxidation methods.

Consequently, several compounds bearing comparable properties were theorized. The feasibility of those molecules, however, still remains to be seen.

6 Use of Artificial Intelligence

This thesis utilized the use of artificial intelligence (ChatGPT, Julius) for more comprehensive understanding of given subjects, grammatical corrections and obtaining out-of-the-box scientific articles. All AI-generated outputs were paid due attention and consideration, and their accuracy was thoroughly investigated before implementing them in this thesis. The use of AI aligns with ethical practices and does not substitute for the author's critical analysis and independent research.

7 Literature

(1) Glockler, G. Carbon–Oxygen Bond Energies and Bond Distances. *J. Phys. Chem.* **1958**, *62* (9), 1049–1054. https://doi.org/10.1021/j150567a006.

(2) Vandermeeren, L.; Leyssens, T.; Peeters, D. Theoretical Study of the Properties of Sulfone and Sulfoxide Functional Groups. *J. Mol. Struct. THEOCHEM* **2007**, *804* (1), 1–8. https://doi.org/10.1016/j.theochem.2006.10.006.

(3) Lindquist, B. A.; Dunning, T. H. The Nature of the SO Bond of Chlorinated Sulfur–Oxygen Compounds. *Theor. Chem. Acc.* **2014**, *133* (2), 1443. https://doi.org/10.1007/s00214-013-1443-8.

(4) Bentley, R. Role of Sulfur Chirality in the Chemical Processes of Biology. *Chem. Soc. Rev.* **2005**, *34* (7), 609–624. https://doi.org/10.1039/B418284G.

(5) Rayner, D. R.; Miller, E. G.; Bickart, P.; Gordon, A. J.; Mislow, K. Mechanisms of Thermal Racemization of Sulfoxides1. *J. Am. Chem. Soc.* **1966**, *88* (13), 3138–3139. https://doi.org/10.1021/ja00965a048.

(6) Wojaczyńska, E.; Wojaczyński, J. Sulfoxides in Medicine. *Curr. Opin. Chem. Biol.* **2023**, *76*, 102340. https://doi.org/10.1016/j.cbpa.2023.102340.

(7) Kollerup Madsen, B.; Hilscher, M.; Zetner, D.; Rosenberg, J. Adverse Reactions of Dimethyl Sulfoxide in Humans: A Systematic Review. *F1000Research* **2019**, *7*, 1746. https://doi.org/10.12688/f1000research.16642.2.

(8) Verheijen, M.; Lienhard, M.; Schrooders, Y.; Clayton, O.; Nudischer, R.; Boerno, S.; Timmermann, B.; Selevsek, N.; Schlapbach, R.; Gmuender, H.; Gotta, S.; Geraedts, J.; Herwig, R.; Kleinjans, J.; Caiment, F. DMSO Induces Drastic Changes in Human Cellular Processes and Epigenetic Landscape in Vitro. *Sci. Rep.* **2019**, *9* (1), 4641. https://doi.org/10.1038/s41598-019-40660-0.

(9) Zager, A. Modulating the Immune Response with the Wake-Promoting Drug Modafinil: A Potential Therapeutic Approach for Inflammatory Disorders. *Brain. Behav. Immun.* **2020**, *88*, 878–886. https://doi.org/10.1016/j.bbi.2020.04.038.

(10) *Armodafinil vs Modafinil Comparison*. Drugs.com. https://www.drugs.com/compare/armodafinil-vs-modafinil (accessed 2025-04-11).

(11) Darwish, M.; Kirby, M.; Hellriegel, E. T.; Robertson, P. Armodafinil and Modafinil Have Substantially Different Pharmacokinetic Profiles Despite Having the Same Terminal Half-Lives. *Clin. Drug Investig.* **2009**, *29* (9), 613–623. https://doi.org/10.2165/11315280-000000000-00000.

(12) Kubota, H.; Kakefuda, A.; Nagaoka, H.; Yamamoto, O.; Ikeda, K.; Takeuchi, M.; Shibanuma, T.; Isomura, Y. Spiro-Substituted Piperidines as Neurokinin Receptor Antagonists. II. Syntheses and NK2 Receptor-Antagonistic Activities of N-[2-Aryl-4-(Spiro-Substituted Piperidin-1'-Yl)Butyl]Carboxamides. *Chem. Pharm. Bull. (Tokyo)* **1998**, *46* (2), 242–254. https://doi.org/10.1248/cpb.46.242.

(13) Nishi, T.; Ishibashi, K.; Takemoto, T.; Nakajima, K.; Fukazawa, T.; Iio, Y.; Itoh, K.; Mukaiyama, O.; Yamaguchi, T. Combined Tachykinin Receptor Antagonist: Synthesis and Stereochemical Structure–Activity Relationships of Novel Morpholine Analogues. *Bioorg.*

Med. Chem. Lett. **2000**, *10* (15), 1665–1668. https://doi.org/10.1016/S0960-894X(00)00324-3.

(14) Legros, J.; Dehli, J. R.; Bolm, C. Applications of Catalytic Asymmetric Sulfide Oxidations to the Syntheses of Biologically Active Sulfoxides. *Adv. Synth. Catal.* **2005**, *347* (1), 19–31. https://doi.org/10.1002/adsc.200404206.

(15) Baralić, K.; Živanović, J.; Marić, Đ.; Bozic, D.; Grahovac, L.; Antonijević Miljaković, E.; Ćurčić, M.; Buha Djordjevic, A.; Bulat, Z.; Antonijević, B.; Đukić-Ćosić, D. Sulforaphane—A Compound with Potential Health Benefits for Disease Prevention and Treatment: Insights from Pharmacological and Toxicological Experimental Studies. *Antioxidants* **2024**, *13* (2), 147. https://doi.org/10.3390/antiox13020147.

(16) National Center for Biotechnology Information. *Alpha-Amanitin*. PubChem. https://pubchem.ncbi.nlm.nih.gov/compound/9543442 (accessed 2025-04-11).

(17) Shin, J. M.; Kim, N. Pharmacokinetics and Pharmacodynamics of the Proton Pump Inhibitors. *J. Neurogastroenterol. Motil.* **2013**, *19* (1), 25–35. https://doi.org/10.5056/jnm.2013.19.1.25.

(18) Chasar, D. W.; Pratt, T. M. A Direct Synthesis of 2- and 4-Hydroxydiaryl Sulfoxides. *Phosphorus Sulfur Relat. Elem.* **1978**, *5* (1), 35–40. https://doi.org/10.1080/03086647808069859.

(19) Wudl, Fred.; Lee, T. B. K. Asymmetric Synthesis of Chiral Sulfoxides. II. Intramolecular Oxygen to Nitrogen Sulfinyl Migration. *J. Am. Chem. Soc.* **1973**, *95* (19), 6349–6358. https://doi.org/10.1021/ja00800a031.

(20) Kupwade, R. V. A Concise Review on Synthesis of Sulfoxides and Sulfones with Special Reference to Oxidation of Sulfides. *J. Chem. Rev.* **2019**, *1* (2), 99–113. https://doi.org/10.33945/SAMI/JCR.2019.1.99113.

(21) Saito, F. A Sulfoxide Reagent for One-Pot, Three-Component Syntheses of Sulfoxides and Sulfinamides. *Angew. Chem. Int. Ed.* **2022**, *61* (52), e202213872. https://doi.org/10.1002/anie.202213872.

(22) Capozzi, M. A. M.; Cardellicchio, C.; Naso, F. Enantioselective Routes to Sulfoxides Based Upon the Use of Carbanionic Leaving Groups. *Eur. J. Org. Chem.* **2004**, *2004* (9), 1855–1963. https://doi.org/10.1002/ejoc.200300497.

(23) Lenstra, D. C.; Vedovato, V.; Ferrer Flegeau, E.; Maydom, J.; Willis, M. C. One-Pot Sulfoxide Synthesis Exploiting a Sulfinyl-Dication Equivalent Generated from a DABSO/Trimethylsilyl Chloride Sequence. *Org. Lett.* **2016**, *18* (9), 2086–2089. https://doi.org/10.1021/acs.orglett.6b00712.

(24) Hojo, M.; Masuda, R.; Saeki, T.; Fujimori, K.; Tsutsumi, S. An Alternative Synthetic Method for Aldehydes. Reaction of Methyl Methylthiomethyl Sulfoxide with Grignard Reagents. *Tetrahedron Lett.* **1977**, *18* (44), 3883–3886. https://doi.org/10.1016/S0040-4039(01)83380-3.

(25) Solladié, G. Asymmetric Synthesis Using Nucleophilic Reagents Containing a Chiral Sulfoxide Group. *Synthesis* **2002**, *1981*, 185–196. https://doi.org/10.1055/s-1981-29378.

(26) Bäckvall, J.-E. Selective Oxidation of Amines and Sulfides. In *Modern Oxidation Methods*; John Wiley & Sons, Ltd, 2004; pp 193–222. https://doi.org/10.1002/3527603689.ch7.

(27) Furia, F. D.; Modena, G.; Seraglia, R. Synthesis of Chiral Sulfoxides by Metal-Catalyzed Oxidation with t-Butyl Hydroperoxide. *Synthesis* **2002**, *1984*, 325–326. https://doi.org/10.1055/s-1984-30829.

(28) Pitchen, P.; Kagan, H. B. An Efficient Asymmetric Oxidation of Sulfides to Sulfoxides. *Tetrahedron Lett.* **1984**, *25* (10), 1049–1052. https://doi.org/10.1016/S0040-4039(01)80097-6.

(29) Komatsu, N.; Hashizume, M.; Sugita, T.; Uemura, S. Catalytic Asymmetric Oxidation of Sulfides to Sulfoxides with Tert-Butyl Hydroperoxide Using Binaphthol as a Chiral Auxiliary. *J. Org. Chem.* **1993**, *58* (17), 4529–4533. https://doi.org/10.1021/jo00069a009.

(30) Gao, J.; Guo, H.; Liu, S.; Wang, M. Efficient Soluble Polymer-Supported Tartrate/Ti Catalyst for Asymmetric Oxidation of Prochiral Sulfides. *Tetrahedron Lett.* **2007**, *48* (48), 8453–8455. https://doi.org/10.1016/j.tetlet.2007.09.169.

(31) Jiang, W.; Hu, M.; Liu, F.; Sun, S. Industrial Production Method of Esomeprazole. CN104496964A, April 8, 2015.

(32) O'Mahony, G. E.; Ford, A.; Maguire, A. R. Asymmetric Oxidation of Sulfides. *J. Sulfur Chem.* **2013**, *34* (3), 301–341. https://doi.org/10.1080/17415993.2012.725247.

(33) Han, J.; Soloshonok, V. A.; Klika, K. D.; Drabowicz, J.; Wzorek, A. Chiral Sulfoxides: Advances in Asymmetric Synthesis and Problems with the Accurate Determination of the Stereochemical Outcome. *Chem. Soc. Rev.* **2018**, *47* (4), 1307–1350. https://doi.org/10.1039/C6CS00703A.

(34) Dai, W.; Shang, S.; Lv, Y.; Li, G.; Li, C.; Gao, S. Highly Chemoselective and Enantioselective Catalytic Oxidation of Heteroaromatic Sulfides via High-Valent Manganese(IV)–Oxo Cation Radical Oxidizing Intermediates. *ACS Catal.* **2017**, *7* (7), 4890–4895. https://doi.org/10.1021/acscatal.7b00968.

(35) Bell, E. L.; Finnigan, W.; France, S. P.; Green, A. P.; Hayes, M. A.; Hepworth, L. J.; Lovelock, S. L.; Niikura, H.; Osuna, S.; Romero, E.; Ryan, K. S.; Turner, N. J.; Flitsch, S. L. Biocatalysis. *Nat. Rev. Methods Primer* **2021**, *1* (1), 46. https://doi.org/10.1038/s43586-021-00044-z.

(36) Sen, S.; Venkata Dasu, V.; Mandal, B. Developments in Directed Evolution for Improving Enzyme Functions. *Appl. Biochem. Biotechnol.* **2007**, *143* (3), 212–223. https://doi.org/10.1007/s12010-007-8003-4.

(37) Kuchner, O.; Arnold, F. H. Directed Evolution of Enzyme Catalysts. *Trends Biotechnol.* **1997**, *15* (12), 523–530. https://doi.org/10.1016/S0167-7799(97)01138-4.

(38) Cherry, J. R.; Fidantsef, A. L. Directed Evolution of Industrial Enzymes: An Update. *Curr. Opin. Biotechnol.* **2003**, *14* (4), 438–443. https://doi.org/10.1016/S0958-1669(03)00099-5.

(39) Reetz, M. T.; Wilensek, S.; Zha, D.; Jaeger, K.-E. Directed Evolution of an Enantioselective Enzyme through Combinatorial Multiple-Cassette Mutagenesis. *Angew. Chem. Int. Ed.* **2001**, *40* (19), 3589–3591. https://doi.org/10.1002/1521-3773(20011001)40:19<3589::AID-ANIE3589>3.0.CO;2-X.

(40) Moskovitz, J.; Weissbach, H.; Brot, N. Cloning the Expression of a Mammalian Gene Involved in the Reduction of Methionine Sulfoxide Residues in Proteins. *Proc. Natl. Acad. Sci.* **1996**, *93* (5), 2095–2099. https://doi.org/10.1073/pnas.93.5.2095.

(41) Tian, J.; Zhou, S.; Chen, Y.; Zhao, Y.; Li, S.; Yang, P.; Xu, X.; Chen, Y.; Cheng, X.; Yang, J. Synthesis of Chiral Sulfoxides by A Cyclic Oxidation-Reduction Multi-Enzymatic Cascade Biocatalysis. *Chem. – Eur. J.* **2024**, *30* (19), e202304081. https://doi.org/10.1002/chem.202304081.

(42) Peng, T.; Cheng, X.; Chen, Y.; Yang, J. Sulfoxide Reductases and Applications in Biocatalytic Preparation of Chiral Sulfoxides: A Mini-Review. *Front. Chem.* **2021**, *9*. https://doi.org/10.3389/fchem.2021.714899.

(43) Lin, Z.; Johnson, L. C.; Weissbach, H.; Brot, N.; Lively, M. O.; Lowther, W. T. Free Methionine-(R)-Sulfoxide Reductase from Escherichia Coli Reveals a New GAF Domain Function. *Proc. Natl. Acad. Sci.* **2007**, *104* (23), 9597–9602. https://doi.org/10.1073/pnas.0703774104.

(44) Pascual, I.; Larrayoz, I. M.; Rodriguez, I. R. Retinoic Acid Regulates the Human Methionine Sulfoxide Reductase A (MSRA) Gene via Two Distinct Promoters. *Genomics* **2009**, *93* (1), 62–71. https://doi.org/10.1016/j.ygeno.2008.09.002.

(45) Kim, H.-Y.; Gladyshev, V. N. Methionine Sulfoxide Reductases: Selenoprotein Forms and Roles in Antioxidant Protein Repair in Mammals. *Biochem. J.* **2007**, *407* (3), 321–329. https://doi.org/10.1042/BJ20070929.

(46) Coudevylle, N.; Antoine, M.; Bouguet-Bonnet, S.; Mutzenhardt, P.; Boschi-Muller, S.; Branlant, G.; Cung, M.-T. Solution Structure and Backbone Dynamics of the Reduced Form and an Oxidized Form of *E. Coli* Methionine Sulfoxide Reductase A (MsrA): Structural Insight of the MsrA Catalytic Cycle. *J. Mol. Biol.* **2007**, *366* (1), 193–206. https://doi.org/10.1016/j.jmb.2006.11.042.

(47) Gand, A.; Antoine, M.; Boschi-Muller, S.; Branlant, G. Characterization of the Amino Acids Involved in Substrate Specificity of Methionine Sulfoxide Reductase A *. *J. Biol. Chem.* **2007**, *282* (28), 20484–20491. https://doi.org/10.1074/jbc.M702350200.

(48) Brennan, L. A.; Kantorow, M. Mitochondrial Function and Redox Control in the Aging Eye: Role of MsrA and Other Repair Systems in Cataract and Macular Degenerations. *Exp. Eye Res.* **2009**, *88* (2), 195–203. https://doi.org/10.1016/j.exer.2008.05.018.

(49) Lim, J. C.; You, Z.; Kim, G.; Levine, R. L. Methionine Sulfoxide Reductase A Is a Stereospecific Methionine Oxidase. *Proc. Natl. Acad. Sci.* **2011**, *108* (26), 10472–10477. https://doi.org/10.1073/pnas.1101275108.

(50) Kantorow, M.; Lee, W.; Chauss, D. Focus on Molecules: Methionine Sulfoxide Reductase A. *Exp. Eye Res.* **2012**, *100*, 110–111. https://doi.org/10.1016/j.exer.2010.09.007.

(51) Brennan, L. A.; Lee, W.; Giblin, F. J.; David, L. L.; Kantorow, M. Methionine Sulfoxide Reductase A (MsrA) Restores α-Crystallin Chaperone Activity Lost upon Methionine Oxidation. *Biochim. Biophys. Acta BBA - Gen. Subj.* **2009**, *1790* (12), 1665–1672. https://doi.org/10.1016/j.bbagen.2009.08.011.

(52) Lee, B. C.; Gladyshev, V. N. The Biological Significance of Methionine Sulfoxide Stereochemistry. *Free Radic. Biol. Med.* **2011**, *50* (2), 221–227. https://doi.org/10.1016/j.freeradbiomed.2010.11.008.

(53) Nosek, V.; Míšek, J. Chemoenzymatic Deracemization of Chiral Sulfoxides. *Angew. Chem. Int. Ed.* **2018**, *57* (31), 9849–9852. https://doi.org/10.1002/anie.201805858.

(54) Nosek, V.; Míšek, J. Enzymatic Kinetic Resolution of Chiral Sulfoxides – an Enantiocomplementary Approach. *Chem. Commun.* **2019**, *55* (70), 10480–10483. https://doi.org/10.1039/C9CC05470G.

(55) Tarallo, V.; Sudarshan, K.; Nosek, V.; Míšek, J. Development of a Simple High-Throughput Assay for Directed Evolution of Enantioselective Sulfoxide Reductases. *Chem. Commun.* **2020**, *56* (40), 5386–5388. https://doi.org/10.1039/D0CC01660H.

(56) *Bordwell pKa Table*. Hans Reich's Collection. Bordwell pKa Table. https://organicchemistrydata.org/hansreich/resources/pka/#kahalide (accessed 2025-03-30).

(57) Dai, W.; Li, J.; Li, G.; Yang, H.; Wang, L.; Gao, S. Asymmetric Epoxidation of Alkenes Catalyzed by a Porphyrin-Inspired Manganese Complex. *Org. Lett.* **2013**, *15* (16), 4138–4141. https://doi.org/10.1021/ol401812h.

(58) Iriuchijima, S.; Sakakibara, T.; Tsuchihashi, G. A Method for the Synthesis of Aldehydes. *Agric. Biol. Chem.* **1976**, *40* (7), 1369–1372. https://doi.org/10.1080/00021369.1976.10862212.

(59) Cui, H.; Wei, W.; Yang, D.; Zhang, Y.; Zhao, H.; Wang, L.; Wang, H. Visible-Light-Induced Selective Synthesis of Sulfoxides from Alkenes and Thiols Using Air as the Oxidant. *Green Chem.* **2017**, *19* (15), 3520–3524. https://doi.org/10.1039/C7GC01416C.

(60) Amos, S. G. E.; Nicolai, S.; Gagnebin, A.; Le Vaillant, F.; Waser, J. Metal-Free Electrophilic Alkynylation of Sulfenate Anions with Ethynylbenziodoxolone Reagents. *J. Org. Chem.* **2019**, *84* (6), 3687–3701. https://doi.org/10.1021/acs.joc.9b00050.

(61) Tranquilino, A.; Andrade, S. R. C. P.; da Silva, A. P. M.; Menezes, P. H.; Oliveira, R. A. Non-Expensive, Open-Flask and Selective Catalytic Systems for the Synthesis of Sulfinate Esters and Thiosulfonates. *Tetrahedron Lett.* **2017**, *58* (13), 1265–1268. https://doi.org/10.1016/j.tetlet.2017.02.025.

(62) Le, L.; Li, S.; Zhang, D.; Yin, S.-F.; Kambe, N.; Qiu, R. Base-Promoted Reactions of Organostibines with Alkynes and Organic Halides to Give Chalcogenated (Z)-Olefins and Ethers. *Org. Lett.* **2022**, *24* (33), 6159–6164. https://doi.org/10.1021/acs.orglett.2c02369.

(63) Suzuki, M.; Kanemoto, K.; Nakamura, Y.; Hosoya, T.; Yoshida, S. Palladium-Catalyzed Sulfinylation of Aryl- and Alkenylborons with Sulfinate Esters. *Org. Lett.* **2021**, *23* (9), 3793–3797. https://doi.org/10.1021/acs.orglett.1c01292.

(64) *2411275-41-5 Substance Detail | CAS SciFinder*. https://scifinder-n.cas.org/searchDetail/substance/6824e3684841fe27d50b80eb/substanceDetails (accessed 2025-05-14).

(65) Bethge, L.; Jarikote, D. V.; Seitz, O. New Cyanine Dyes as Base Surrogates in PNA: Forced Intercalation Probes (FIT-Probes) for Homogeneous SNP Detection. *Bioorg. Med. Chem.* **2008**, *16* (1), 114–125. https://doi.org/10.1016/j.bmc.2006.12.044.